iScience

CellPress
OPEN ACCESS

Article

Distinct effects of AMPAR subunit depletion on spatial memory

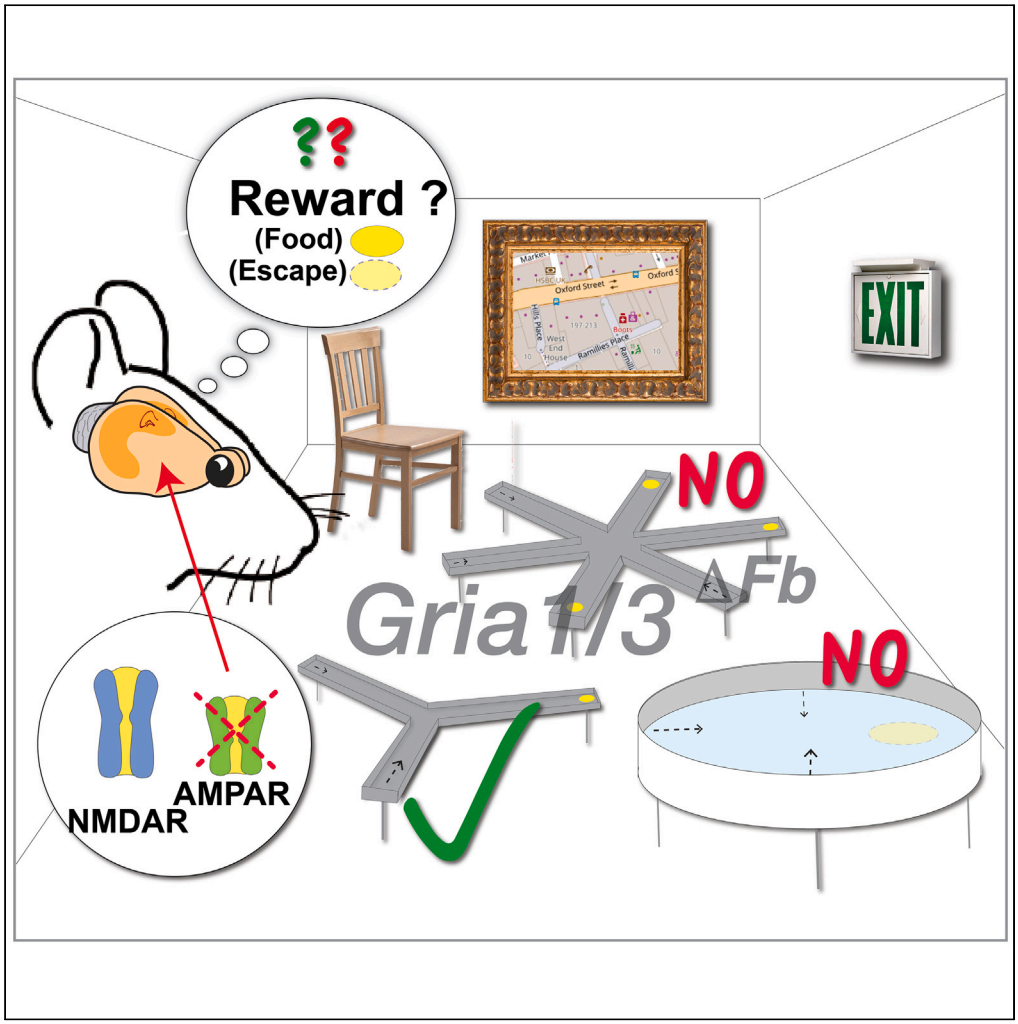

Ahmed Eltokhi, Ilaria Bertocchi, Andrei Rozov, ..., John Nick P. Rawlins, David M. Bannerman, Rolf Sprengel

david.bannerman@psy.ox.ac.uk (D.M.B.)
sprengel@mr.mpg.de (R.S.)

Highlights

Severely reduced AMPAR responses are life-threatening in new born mice

Lack of GluA1/A3 is associated with reduced hippocampal GluA2 and increased GluN2A

The reduced hippocampal EPSCs in *Gria1/3*$^{-/-}$ mice depend on NMDA/KA receptors

There is redundancy of iGluR function for long-term spatial memory performance

Eltokhi et al., iScience *26*, 108116
November 17, 2023
https://doi.org/10.1016/j.isci.2023.108116

iScience

CellPress
OPEN ACCESS

Article

Distinct effects of AMPAR subunit depletion on spatial memory

Ahmed Eltokhi,[1,2] Ilaria Bertocchi,[1,3,4] Andrei Rozov,[1,5,6] Vidar Jensen,[7] Thilo Borchardt,[1] Amy Taylor,[8] Catia C. Proenca,[1] John Nick P. Rawlins,[8] David M. Bannerman,[8,*] and Rolf Sprengel[1,9,*]

SUMMARY

Pharmacological studies established a role for AMPARs in the mammalian forebrain in spatial memory performance. Here we generated global GluA1/3 double knockout mice (*Gria1/3*$^{-/-}$) and conditional knockouts lacking GluA1 and GluA3 AMPAR subunits specifically from principal cells across the forebrain (*Gria1/3*$^{\Delta Fb}$). In both models, loss of GluA1 and GluA3 resulted in reduced hippocampal GluA2 and increased levels of the NMDAR subunit GluN2A. Electrically-evoked AMPAR-mediated EPSPs were greatly diminished, and there was an absence of tetanus-induced LTP. *Gria1/3*$^{-/-}$ mice showed premature mortality. *Gria1/3*$^{\Delta Fb}$ mice were viable, and their memory performance could be analyzed. In the Morris water maze (MWM), *Gria1/3*$^{\Delta Fb}$ mice showed profound long-term memory deficits, in marked contrast to the normal MWM learning previously seen in single *Gria1*$^{-/-}$ and *Gria3*$^{-/-}$ knockout mice. Our results suggest a redundancy of function within the pool of available ionotropic glutamate receptors for long-term spatial memory performance.

INTRODUCTION

L-α-amino-3-hydroxy-5-methyl-4-isoxazolepropionic acid receptors (AMPARs) support the majority of fast, excitatory synaptic transmission in the mammalian forebrain. Moreover, the process by which AMPAR trafficking is stimulated and directed toward active synaptic zones underlies synaptic plasticity in many brain regions.[1,2] In the hippocampus, it is well documented that fast glutamatergic transmission plays a key role in learning and memory. For instance, the infusion of broad spectrumAMPAR/KainateR antagonists, LY326325, CNQX or NBQX, into the hippocampus impairs spatial memory performance in the Morris water maze (MWM).[3] This impairment is observed when the antagonists are infused prior to training as well as when they are administered before recall in pre-trained rats.[4] Despite the long-standing realization that spatial memory depends on AMPA/Kainate transmission, the contribution of different AMPAR subunits to long-term spatial memory performance has remained elusive.

Together with N-methyl-D-aspartate receptors (NMDARs) and Kainate receptors (KARs), AMPARs form the family of ionotropic glutamate receptors (iGluRs). Members of all three subfamilies are encoded by their own genes which are differentially expressed in different brain regions during development and in the adult brain.[5–7] In the case of the AMPAR family, the GluA1, A2, A3 and A4 subunits are involved in the formation of a tetrameric ligand-gated ion channel. The subunits GluA1, 2 and 3 form the AMPAR core complex in excitatory cells in various combinations. The majority of these AMPARs, at least in hippocampal excitatory neurons, are Ca^{2+}-impermeable and are formed after the tetramerization of two GluA1/GluA2 dimers or tetramerization of two GluA2/GluA3 dimers in native ER membranes during secretion.[8,9] The homomeric Q/R site-edited GluA2 and homomeric GluA3 receptors can be formed *in vivo* but are poorly transported to the plasma membrane and thus to synapses.[10–12] In the mature brain, the Q/R site- edited GluA2 subunit "GluA2(R)" is the most abundant GluA2 isoform.[13] GluA2(R) determines critically the Ca^{2+}-impermeability of GluA2-containing AMPARs. In contrast, GluA4-containing AMPARs are Ca^{2+}-permeable. GluRA4 is expressed together with GluA1 and/or GluA3 mainly in the cerebellum, olfactory bulb and interneurons, and only transiently during development in CA1 pyramidal neurons.[6,14–16] GluA4 global knockout had no effect on associative long-term spatial memory performance in the MWM[17] but showed a mild impairment in spatial learning in the Barnes Maze.[18]

Gria3$^{-/-}$ global knockout mice exhibited several phenotypes,[19–21] while maintaining normal synaptic transmission with enhanced LTP[22] and regular long-term spatial reference memory performance in the MWM[21] [for review, see: Italia at al., 2021[23]]. In contrast, both global

[1]Departments of Molecular Neurobiology and Physiology, Max Planck Institute for Medical Research, Heidelberg, Germany
[2]Department of Pharmacolog, University of Washington, Seattle, WA, USA
[3]Department of Neuroscience Rita Levi Montalcini, University of Turin, 10126 Turin, Italy
[4]Neuroscience Institute - Cavalieri-Ottolenghi Foundation (NICO), Laboratory of Neuropsychopharmacology, Regione Gonzole 10, Orbassano, 10043 Torino, Italy
[5]Institute of Neuroscience, Lobachevsky State University of Nizhniy, 603022 Novgorod, Russia
[6]Federal Center of Brain Research and Neurotechnology, 117997 Moscow, Russia
[7]Department of Molecular Medicine, Division of Physiology, Institute of Basic Medical Sciences, University of Oslo, 0372 Oslo, Norway
[8]Department of Experimental Psychology, University of Oxford, Oxford, UK
[9]Lead contact
*Correspondence: david.bannerman@psy.ox.ac.uk (D.M.B.), sprengel@mr.mpg.de (R.S.)
https://doi.org/10.1016/j.isci.2023.108116

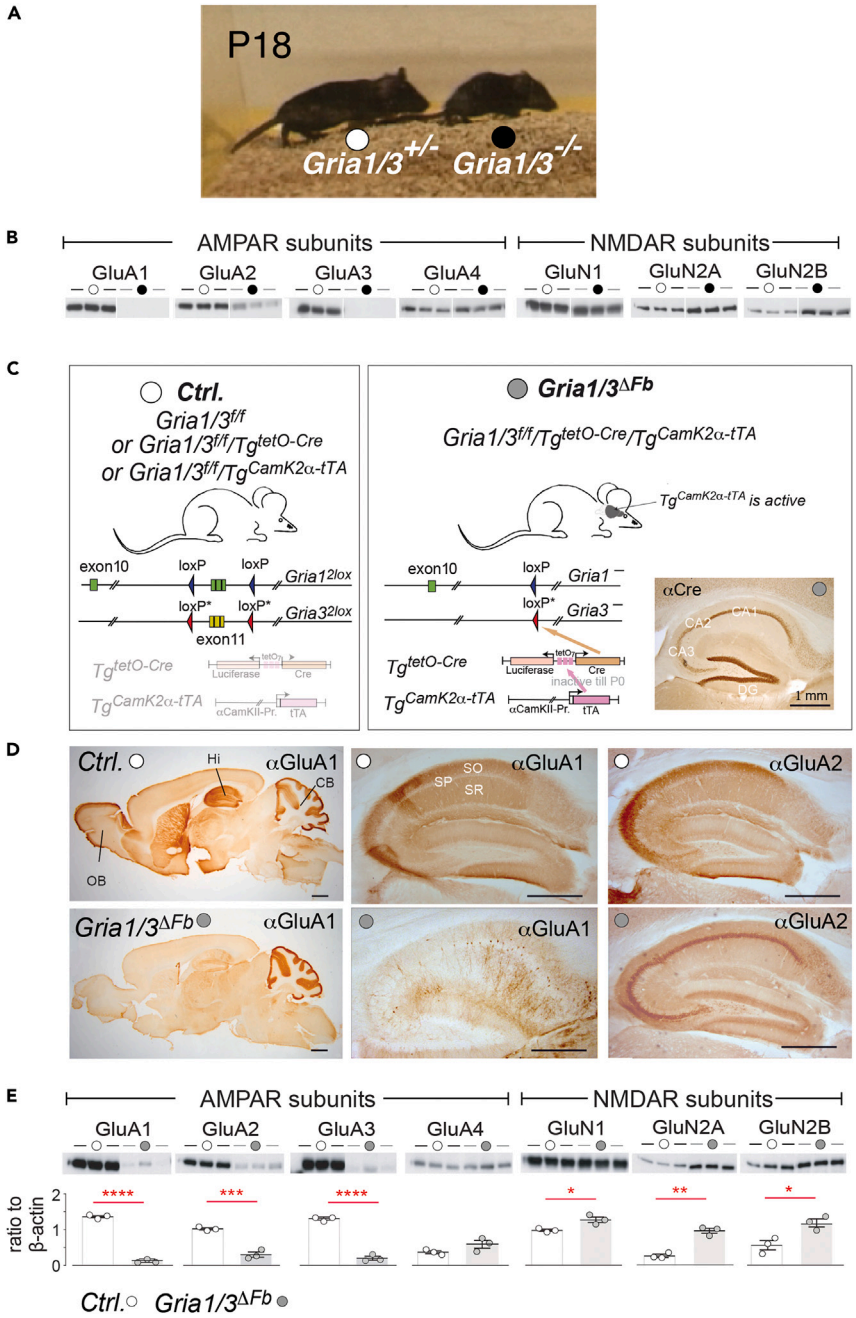

Figure 1. Generation and molecular analysis of global double GluA1 and GluA3 knockout mice (*Gria1/3*$^{-/-}$) and constitutive mutants (*Gria1/3*$^{\Delta Fb}$) with specific loss of the GluA1 and GluA3 subunits in excitatory forebrain neurons

(A) *Gria1/3*$^{-/-}$ were generated by matings of GluA1 and GluA3 knockout mice. A three-week-old *Gria1/3*$^{-/-}$ mouse raised by a foster mother can be recognized by its smaller body size and impaired body behavior in comparison to a *Gria1/3*$^{-/+}$ littermate (see: Video S1).

(B) Immunoblot analyses of hippocampal extracts for all four members of the AMPAR family evidenced the depletion of GluA1 and GluA3, and a decrease in GluA2 level accompanied by a trend toward increased GluN2A and GluN2B in *Gria1/3*$^{-/-}$ mice (for immunoblots and MW size marker see Figure S4).

(C) Generation of *Gria1/3*$^{\Delta Fb}$ mice: The transgenic encoded transcription factor tTA expressed by the promoter of the alpha subunit of the αCamKII gene (αCamkII-Pr.) was used to drive the expression of the transgenic Cre recombinase in excitatory neurons of the forebrain, as monitored by the immunohistological analysis of Cre expression (right inset) of the transgene (*Tg*$^{tetO\text{-}Cre}$) in the hippocampus (CA1,2,3 Cornu Ammunis layer 1,2,3; DG = Dentate Gyrus). After integrating *Tg*$^{CamkIIa\text{-}tTA}$ and *Tg*^{tetOCre} transgenes into the genetic background of mice encoding the floxed *Gria1*^{2lox} [*Gria1*$^{f/f}$ (*loxP* sites)] and floxed *Gria3*^{2lox} [*Gria3*^{ff} (*LoxP** = *loxP*7151 sites)] genes, we obtained *Gria1/3*$^{\Delta Fb}$ mice with the forebrain-specific gene deletion of the exon 11 in the *Gria1* and *Gria3* gene regions encoding the essential transmembrane spanning region M1 and the channel pore loop fragment P2 (indicated as black bars in the in exon 11) in both *Gria* genes.

Figure 1. *Continued*

(D) The depletion of GluA1-containing AMPARs could be monitored by the massive loss of GluA1 immunoreactivity in the forebrain and hippocampus of *Gria1/3*$^{\Delta Fb}$ mice and by the accumulation of the GluA2 subunit in the cellular layers when compared to controls. (DG = Dentate Gyrus, Hi = Hippocampus, CB = Cerebellum, SO = Stratum Oriens, SP = Stratum pyramidale, SR = Stratum Radiatum). (E) The quantitative immunoblot analyses of hippocampal extracts for all four members of the AMPAR family showed a significant reduction of those subunits which are expressed in excitatory hippocampal neurons; GluA1, GluA2 and GluA3, and a significant increase of GluN1, GluN2A and GluN2B in *Gria1/3*$^{\Delta Fb}$ mice. In (B) and (E), the statistical analysis was performed using the unpaired Student's *t* test. *p $\leq$ 0.05, **p $\leq$ 0.01, ***p $\leq$ 0.001, ****p $\leq$ 0.0001. Error bars indicate the standard error of the mean (SEM). (For the size markers of immunoblots in Figures 1 B and 1E, see Figure S6).

Gria2$^{-/-}$ and *Gria2/3*$^{-/-}$ knockout mice were not suitable for the study of hippocampal-dependent learning due to their motor coordination problems, reduced exploration and increased mortality.[22,24]

Although GluA1, together with GluA2, is the most prominent subunit of the AMPAR population in principle hippocampal neurons,[25] the whole-brain genetic depletion of GluA1 did not have any effect on long-term spatial memory when tested on the standard fixed location, hidden escape platform, reference memory version of the MWM task.[26] Still, these mice were found to exhibit a selective short-term memory impairment,[27,28] and have been discussed as a putative animal model for schizophrenia-like phenotypes.[29–31] In our most recent publication, we showed that the impaired short-term memory in a GluA1 knockout mouse is a key driver of enhanced striatal dopamine responses, which may be an important contributor to aberrant salience and psychosis.[32]

Using our conditional GluA1 knockout mice (*Gria1*$^{f/f}$), we were able to allocate these behavioral phenotypes to the hippocampus using CRE expression by viruses or transgenes.[33,34] Despite the presence of normal spatial learning in the MWM, tetanic stimulation of CA3-to-CA1 synapses in GluA1 knockout mice could not induce the classical field LTP. However, with alternative stimulation procedures that rely on the massive depolarization of the postsynaptic cell during presynaptic input signals, such as "Pairing" or "Theta-burst-stimulation," the activity-induced enhancement of CA3-to-CA1 synaptic transmission could be achieved.[35–37] Thus, it appears that the traditional field LTP seems, in particular, to rely on a pool of extrasynaptic GluA1-containing AMPARs.[38]

The generation and analysis of region-specific and conditional AMPAR depletion in excitatory forebrain neurons or specific parts of the hippocampus using mice with floxed *Gria* genes (*GriaX*$^{f/f}$) provides a more differentiated picture of the function of the AMPAR in synaptic plasticity and spatial learning. Mice with a forebrain-specific GluA2 depletion (*Gria2*$^{\Delta Fb}$ mice) from pyramidal cells showed some enhancement of the Theta-burst-induced LTP, exhibited a spatial working memory deficit and only a mild spatial reference memory impairment in an appetitively motivated Y-maze task, suggesting residual spatial memory performance in these animals.[39] This residual memory persisted, even in the absence of the GluA1 and GluA2 subunits in *Gria1*$^{-/-}$/*2*$^{\Delta Fb}$ mice, with a 5- to 10-fold reduction of AMPAR currents in the hippocampus,[40] suggesting that the AMPAR currents, mediated by the putative remaining Ca^{2+} -permeable GluA3 homomers at hippocampal CA1 synapses, might be sufficient for simple forms of long-term spatial memory.

In wildtype mice, Lu et al.,[41] estimated by employing our conditional triple knockout *Gria1/2/3*$^{f/f}$ mice that about 81% and 16% of synaptic AMPARs in excitatory synapses are composed of GluA1/2 and GluA2/3 receptors, respectively. The remaining 3% of receptors could not be identified as any particular AMPAR subtype, and ~95% of the currents at somatic outside-out patches were supported by GluA1/2 heteromers.[41] The very low numbers of GluA1-type receptors that contain GluA3 subunits, as determined in our Co-IP studies,[42] could potentially originate from hippocampal interneurons. Hippocampal interneurons are well known to co-express GluA1, 3 and 4.[17,43] In addition, the number of synaptic and extrasynaptic GluA2/3 receptors might be underestimated since the channel function of GluA2/3 receptors is inactive under basal conditions.[44]

To explore whether, in the absence of GluA1/2 and GluA2/3 receptors, residual synaptic transmission in excitatory neurons is sufficient for learning, we generated global and conditional GluA1/3 knockout mice (*Gria1/3*$^{-/-}$; *Gria1/3*$^{\Delta Fb}$) and analyzed the basic molecular, histological, and behavioral phenotypes of both mouse models. In particular, we were interested in spatial memory performance, since neither the single GluA1 nor single GluA3 knockout mice had any deficit in long-term spatial memory,[21,26] and the fact that GluA1/2 and GluA2/3 type receptors constitute the entire population of the hippocampal synaptic AMPARs. Therefore, long-term memory performance was assessed in conditional *Gria1/3*$^{\Delta Fb}$ mice across a battery of hippocampus-dependent, spatial memory tests. The performance of hippocampal-lesioned mice, known to be deficient across a wide range of spatial memory tasks,[45] was tested alongside the *Gria1/3*$^{\Delta Fb}$ mice at the same time.

RESULTS

Generation and analysis of global *Gria1/3* knockout mice

We first generated whole-brain GluA1/3 knockout animals (*Gria1/3*$^{-/-}$) by crossing *Gria1*$^{-/-}$[26] with *Gria3*$^{-/-}$ mice,[21] and offspring were genotyped by tail biopsies as described.[21,26] The observed number of born GluA1/3 double-knockout mice was consistent with the expected Mendelian ratio (1/16), suggesting no embryonic lethality for the double-knockout mice. However, we noticed that *Gria1/3*$^{-/-}$ mice were smaller, had to be nursed by foster mothers, and adolescent mice required a calory-rich diet. Nevertheless, *Gria1/3*$^{-/-}$ mice remained significantly smaller than control littermates and phenotypically noticeably weakened (Figure 1A, and Video S1). In preliminary open field and rotarod tests, 3 months old *Gria1/3*$^{-/-}$ mice performed poorly (Figures S1A and S1B), although histological analysis of their brains showed no obvious abnormalities in brain structure and CNS anatomical organization (Figure S2). Additionally, *Gria1/3*$^{-/-}$ mice and control mice had similar marker protein distribution e.g., NeuN and GluN1 with the exception of the accumulation of GluA2 in the cellular layers of the hippocampus (*Str. pyramidale and granule cell layer of the DG*) (Figure S3) as previously described in *Gria1*$^{-/-}$ mice.[26,46] This can be considered a characteristic sign of the trafficking issue of putative GluA2 homomers in hippocampi.[10,47,48] In the cerebellum, the distribution of GluA2

immunohistochemical signal was comparable between controls and *Gria1/3*$^{-/-}$ mice (Figure S3B) despite the complete absence of GluA1 and GluA3 in cerebellar extracts (Figure S4).

Quantitative immunoblots of *Gria1/3*$^{-/-}$ mice showed that neither GluA1 nor GluA3 was expressed in the hippocampus (Figure 1B), cerebellum or cortex (Figure S4) and that the accumulation of the GluA2 immunosignal in the cellular layer of the hippocampus was associated with a reduced GluA2 immunoblot signal, suggesting a degradation of the unassembled GluA2 subunits that reside in an intracellular pool in the endoplasmic reticulum.[49] Reduced GluA2 levels were also noticed to some extent in the cerebellum of *Gria1/3*$^{-/-}$ mice although the immunohistological GluA2 distribution in the cerebellum was similar to controls (Figure S3B). This may suggest that rules for the transport of GluA2 receptor components and thus the AMPAR-associated proteins in the cerebellum are different from the very well-studied hippocampal trafficking, as might be indicated for the GluA3-dependent LTP at Purkinje cells.[50] In addition, there was a trend toward increased GluN2A and GluN2B levels in the hippocampus (Figure 1B), a trend which was less pronounced in the cortex and cerebellum (Figure S4).

Generation and analysis of forebrain-restricted *Gria1/3* knockout mice

To specifically assess learning behavior that is mediated by excitatory forebrain neurons, and to avoid behavioral impairments observed in the global GluA1/2- and GluA1/3-deficient mice, we generated conditional *Gria1/3*$^{\Delta Fb}$ mice with *Gria1* and *Gria3* gene deletions restricted to excitatory neurons of the forebrain, by using mice with *loxP* site flanked *Gria1*$^{f/f}$ alleles and *Gria3*$^{f/f}$ alleles (see Figure S5 for the description of the floxed *Gria1*^{f} allele), in combination with a transgenic mouse expressing Cre recombinase, controlled by the well-characterized transgenic αCaMKII promoter fragment [e.g.,[51–54]] specifically in excitatory neurons of the forebrain (Figure 1C). *Gria1/3*$^{\Delta Fb}$ mice were viable and suitable for complex phenotyping. The immunohistological staining of coronal *Gria1/3*$^{\Delta Fb}$ brain sections showed that the expected strong Cre expression in all cellular layers of the hippocampus (Figure 1C) was accompanied by a strongly reduced GluA1 immunohistological signal in the forebrain (Figure 1D). Only a minor population of neurons in the CA1 region, probably interneurons, was still GluA1 positive. The typical intense GluA1 immunohistological signal in the hippocampal neuropil was not present in *Gria1/3*$^{\Delta Fb}$ mice (Figure 1D). The hippocampal GluA2 signal was accumulated in the cellular hippocampal layers (*Str. pyramidale and granule cell layer of the DG*) of *Gria1/3*$^{\Delta Fb}$ (Figure 1D) as described for the global *Gria1/3*$^{-/-}$ knockout mice (Figure S3). The drastically reduced GluA1, 3 and reduced GluA2 levels in the hippocampi of *Gria1/3*$^{\Delta Fb}$ mice could be verified in quantitative immunoblots. A trend toward increased levels of GluN2A and GluN2B levels in *Gria1/3*$^{-/-}$ knockout mice reached significance in the hippocampi of *Gria1/3*$^{\Delta Fb}$ mice (Figures 1E and S6).

L-α-amino-3-hydroxy-5-methyl-4-isoxazolepropionic acid receptors currents and tetanic field LTP are absent in CA1 principal cells

We next investigated the effect of combined GluA1 and GluA3 deletion on the amplitude of AMPAR-mediated spontaneous excitatory postsynaptic currents (sEPSCs) in CA1 pyramidal cells of brain slices from *Gria1/3*$^{-/-}$ mice at postnatal day 14 (P14) in the presence of Mg^{2+} to block NMDAR-mediated currents. While in control animals sEPSC were relatively frequent (IEI: 0.72 ± 0.12 s n = 5) and had a mean amplitude of 27 ± 11 pA, we did not observe any detectable sEPSC events in slices from age-matched *Gria1/3*$^{-/-}$ mice although the threshold of detection was set 2 times higher than the noise level (Figure 2A), suggesting a very strong reduction or absence of AMPA-currents in CA1 cells of *Gria1/3*$^{-/-}$ mice. Another common way to assess the consequences of genetic manipulations on the functional expression of AMPAR and NMDAR channels is the analysis of induced excitatory postsynaptic currents (EPSCs) in absence of Mg^{2+}. EPSCs recorded in *Gria1/3*$^{-/-}$ mice were mediated almost exclusively by D-APV sensitive iGluRs and were therefore classified as NMDARs (Figure 2B, left). The fast component of the EPSC that remained after blocking NMDAR channels by NBQX was very small (7 ± 1.6 pA) and also insensitive to the application of 50 μM of AMPAR selective antagonist GYKI (6.8 ± 0.83 pA; n = 5; p > 0.05), suggesting the contribution of KAR channels. This very low contribution of AMPA/Kainate iGluRs to the fast excitatory synaptic transmission in *Gria1/3*$^{-/-}$ mice persists in adulthood and could be observed in mice at P42 (Figure 2B, right). The contribution of KAR channels finds support by the analysis of the field excitatory postsynaptic potentials (fEPSPs) at CA3-to-CA1 synapses in hippocampal slices. As expected, in the presence of the AMPAR/KAR blocker, NBQX, the recorded fEPSP response in CA1 to an electrical stimulation of the CA3 fibers in the *str. radiatum* was completely switched off in both *Gria1*$^{-/-}$ and *Gria3*$^{-/-}$ mice, and was not affected by the NMDAR blocker D-APV (Figure S7A). However, in *Gria1/3*$^{-/-}$ double knockout mice, a slower fEPSP response could only be partially blocked by either NBQX or D-APV (Figure S7A). This revealed a partly operative NMDAR and a KAR component, that could also be detected in cellular EPSPs (Figure S7B), in principle neurons when GluA1 and GluA3 subunits are simultaneously depleted.

To evaluate whether this residual fEPSP can be modulated in an activity-dependent manner, we measured hippocampal CA3-to-CA1 field LTP in hippocampal slices from *Gria1/3*$^{-/-}$ and *Gria1/3*$^{\Delta Fb}$ mice. When we stimulated the inputs to CA1 pyramidal cells of adult animals by tetanic stimulation, no potentiation of CA1 field responses could be detected, neither in young *Gria1/3*$^{-/-}$ nor in adult *Gria1/3*$^{\Delta Fb}$ mice (Figure 2C). In adult control mice, the tetanic stimulation of the afferent fibers produced a persistent potentiation of the synaptic responses, characteristic of LTP. The average fEPSP slope 40–45 min after tetanization was 129% ± 4% (mean ± SEM) of the normalized pre-tetanic control value, whereas synaptic transmission in the control pathway was unchanged (98% ± 2%). In contrast, in adult conditional *Gria1/3*$^{\Delta Fb}$ mice, the tetanic stimulation gave a non-significant increase of fEPSPs responses in the *str. radiatum* from 100% ± 3% (control pathway) to 105% ± 3% in the tetanized pathway, indicating the lack of a tetanus-induced change of the synaptic strength in absence of GluA1 and GluA3 at those synapses in *Gria1/3*$^{\Delta Fb}$ mice (Figure 2C).

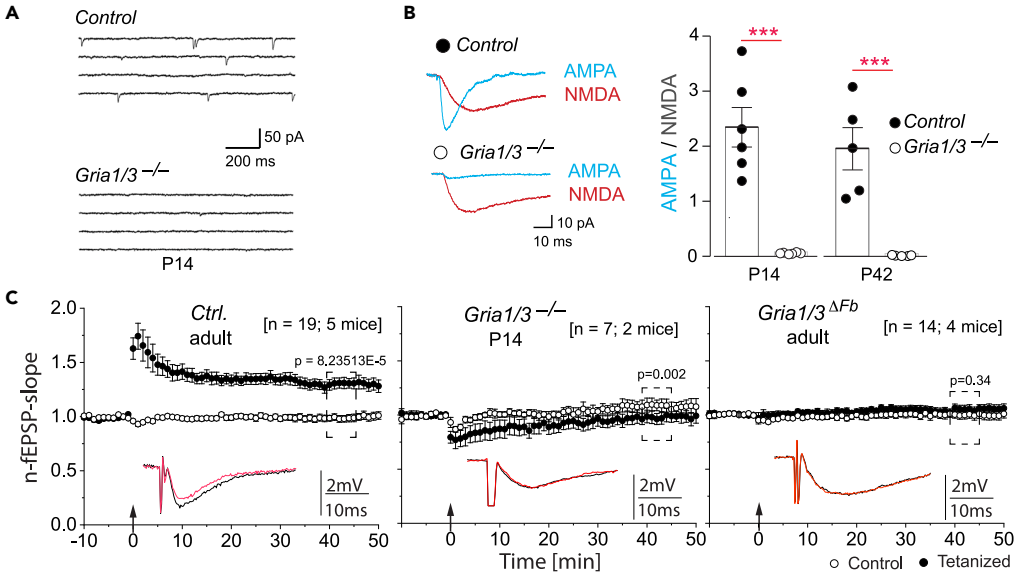

Figure 2. Alterations in synaptic transmission and synaptic plasticity at the hippocampal synapse in the absence of GluA1 and GluA3

(A) Spontaneous EPSCs in CA1 pyramidal neurons were recorded from brain slices of 4 control mice at a holding potential of −70 mV in the presence of 1 mM Mg^{2+} at postnatal day 14. In the bottom panel, examples of continuous recordings under the same conditions in 4 *Gria1/3*$^{-/-}$ mice are depicted. Note the absence of any detectable spontaneous EPSCs in *Gria1/3*$^{-/-}$ mice.

(B) AMPA/NMDA ratios were measured from electrically evoked EPSCs in CA1 pyramidal cells in Mg^{2+}-free ACSF in control and *Gria1/3*$^{-/-}$ mice. The left panel shows example traces of pharmacologically isolated putative NMDA and AMPA currents. The left panel shows example traces of pharmacologically isolated NBQX-resistant and D-APV-resistant currents named as putative NMDA and AMPA currents, respectively. The right panel compares AMPA/NMDA ratios from young and adult control and *Gria1/3*$^{-/-}$ mice. In both groups, the ratios measured in *Gria1/3*$^{-/-}$ mice were significantly smaller relative to values obtained for control animals (***$p < 0.001$, t-test).

(C) Field LTP recordings at CA3/CA1 synapses in the different genotypes as indicated. LTP was quantified by the mean slope taken 40–45 min after tetanization. In hippocampal slices of *Gria1/3*$^{-/-}$ mice at P14, the EPSPs were reduced after tetanic stimulation, and in adult *Gria1/3*$^{\Delta Fb}$ conditional knockout mice, the LTP was abolished. The time points of the tetanization (100Hz for 1 s) are indicated by arrows. The numbers of slices and animals used for the recordings are indicated. Open symbols show the control pathway, and filled symbols show the tetanized pathway. Mean of six consecutive EPSPs just before tetanization (red) and 40 min after (black) are inserted into the result panels. Representative traces before (red) and after (black) are given in as insets.

Preliminary behavioral analysis of *Gria1/3*$^{\Delta Fb}$ mice

To analyze the behavioral consequences of the altered synaptic signaling and its lack of activity-induced modulation by tetanic stimulation, we used *Gria1/3*$^{\Delta Fb}$ mice (i) due to the severe behavioral impairments of global *Gria1/3*$^{-/-}$ knockout mice and (ii) to keep the focus on the function of AMPAR in excitatory neurons in the forebrain. The visual inspection of the *Gria1/3*$^{\Delta Fb}$ mice in their home cages did not reveal any gross abnormalities. However, there was a reduction in body weights and grip strength in the wire-hanging test (Figures 3A and 3B; Table S1). *Gria1/3*$^{\Delta Fb}$ mice displayed a deficit in nesting behavior and exhibited reduced burrowing in the first 2 h of the test, whereas the levels of burrowing overnight were not impaired (Table S1).

Further assessment across a battery of tests revealed a number of phenotypes in *Gria1/3*$^{\Delta Fb}$ mice. For example, *Gria1/3*$^{\Delta Fb}$ mice displayed an impairment in the multiple static rods tests despite their normal performance on the horizontal bar (Table S2). They demonstrated normal motor learning on the rotarod across 5 days of testing (3 trials per day) [Main effect of genotype: $F(1, 21) = 2.514$; $p = 0.1278$; genotype by trial interaction: $F(14, 294) = 0.4836$; $p = 0.9411$] (Figure 3C). In a 2 h assessment of spontaneous locomotor activity using photobeam breaks, *Gria1/3*$^{\Delta Fb}$ mice displayed long-lasting hyperactivity (Figure 3D; and Table S1). In a 5 min open field test in a bigger novel unpleasant environment, the distance traveled by *Gria1/3*$^{\Delta Fb}$ was highly variable across *Gria1/3*$^{\Delta Fb}$ mice (although not different overall from controls), whereas the number of rearings was consistently reduced in *Gria1/3*$^{\Delta Fb}$ mutants (Figure 3E). There were no overt differences in anxiety levels between *Gria1/3*$^{\Delta Fb}$ and control mice on several ethological, unconditioned tests of anxiety, e.g., light/dark box, food hyponeophagia, and the successive alleys test which is a modified version of the elevated plus maze (Figure 3F; and Table S1). As expected from the emotional learning deficits in GluA1 knockout mice,[55,56] *Gria1/3*$^{\Delta Fb}$ mice displayed a pronounced deficit on the passive avoidance test when tested 24 h after conditioning (Figure 3G). A similar impairment was previously correlated with a selective absence of GluA1-dependent LTP in the basolateral amygdala.[56]

Spatial memory performance in *Gria1/3*$^{\Delta Fb}$ mice

Given the role of the hippocampus in spatial memory[57–59] and the altered synaptic transmission and plasticity at hippocampal CA3-to-CA1 synapses in *Gria1/3*$^{\Delta Fb}$ mice, we aimed at testing whether the previously reported impaired GluA1-dependent spatial working memory[27] will

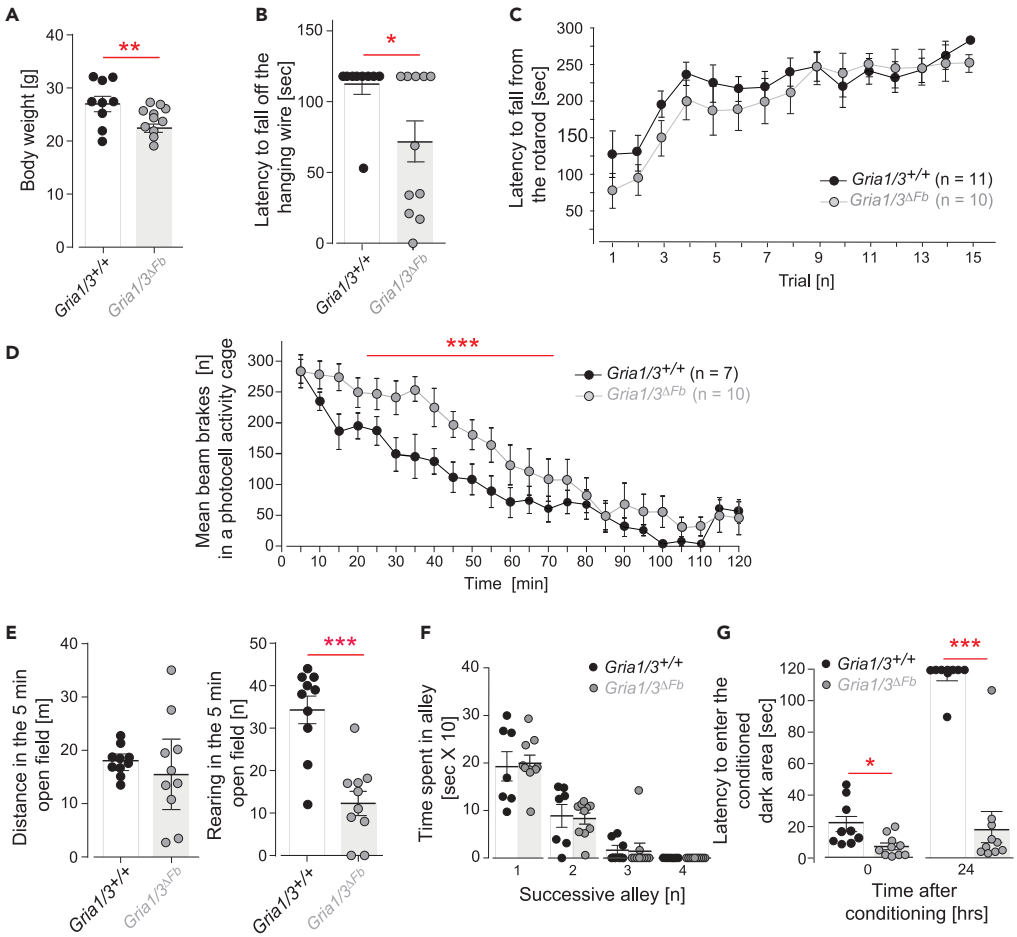

Figure 3. General performance, motor skills and exploratory activities of *Gria1/3*$^{\Delta Fb}$ mice

(A) The body weight of *Gria1/3*$^{\Delta Fb}$ mice was significantly reduced.

(B) The latency to fall from the hanging wire was decreased in *Gria1/3*$^{\Delta Fb}$ mice.

(C) *Gria1/3*$^{\Delta Fb}$ showed robust rotarod learning across 15 trials.

(D) Increased activity of *Gria1/3*$^{\Delta Fb}$ mice in a 2 h spontaneous locomotor activity test measured by the mean number of beam breaks per group in photocell activity cage.

(E) In the 5 min open field test, the distance traveled was highly variable in *Gria1/3*$^{\Delta Fb}$ mice (Mann Whitney U test was non-significant ($p = 0.436$), and rearing was significantly reduced in *Gria1/3*$^{\Delta Fb}$ mice (Mann Whitney U test ***$p < 0.001$; median +/− IQR).

(F) In the successive alleys, there was no difference in the time spent by the *Gria1/3*$^{\Delta Fb}$ or the control mice in each of the alleys in the successive alleys. The graph shows the mean time spent in seconds for each group of animals in each of the alleys.

(G) In the passive avoidance fear conditioning test, a significant learning impairment could be observed in *Gria1/3*$^{\Delta Fb}$ mice. In (A), (B), (D), (F)and (G), the SEM are given *$p \leq 0.05$, **$p \leq 0.01$, ***$p \leq 0.001$.

be accompanied by a deficit in spatial reference memory in our double knockout mice. In a battery of hippocampus-dependent spatial memory tasks, we compared control, *Gria1/3*$^{\Delta Fb}$ and hippocampal-lesioned mice with almost complete destruction of the hippocampus [see: Supplementary information in Bannerman et al., 2012[45]].

Y-maze spatial reference memory task

First, we assessed associative spatial memory using an appetitively motivated, reference memory Y-maze task in which one arm of the maze (defined by the allocentric, extramaze cues) was consistently associated with a milk reward (Figure 4A). While the sham-lesioned animals readily acquired this task, the hippocampal-lesioned mice showed little, if any, improvement across the eleven days of training. *Gria1/3*$^{\Delta Fb}$ mice and their controls learned the task at the same rate. After 100 trials, the controls, shams and knockout animals had all acquired the task to a very high level of performance but the hippocampal-lesioned animals remained at near-chance levels of performance. ANOVA revealed a main effect of group [$(F (3, 30) = 44.51; p < 0.0001)$], a main effect of day [$F (9, 270) = 44.14; p < 0.0001$] and groups by days interaction [$F (27, 270) = 5.6; p < 0.0001$]. Analysis of simple main effects confirmed group differences from day 3 onwards [$F (3,251) = 7.26; p < 0.001$].

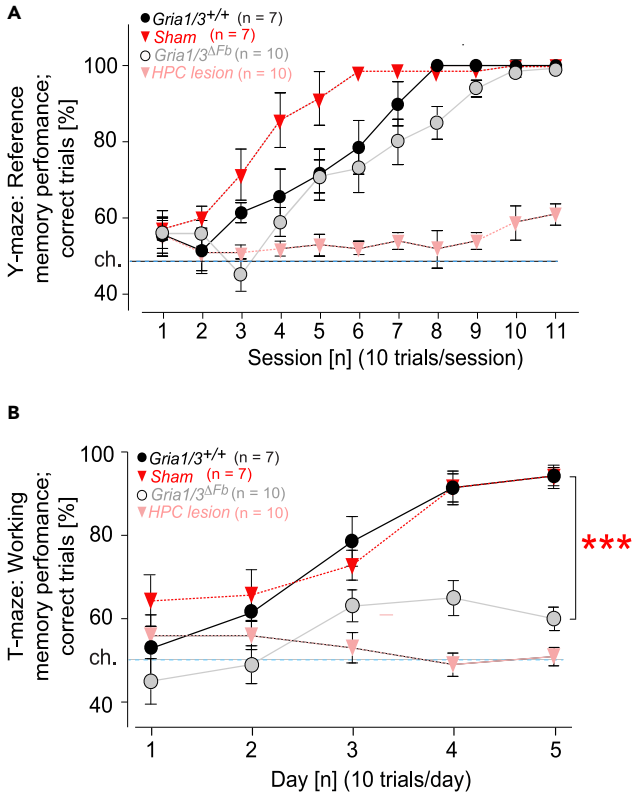

Figure 4. Y and T-maze performance of *Gria1/3*$^{\Delta Fb}$ and hippocampal-lesioned mice

(A) *Gria1/3*$^{\Delta Fb}$ mice were able to acquire the Y-maze spatial reference memory task as well as their littermate controls. Mice with hippocampal lesions were impaired on this task, while the sham-operated animals acquired the task more quickly than the *Gria1/3*$^{\Delta Fb}$ mice and the control mice. The figure shows mean correct choices (±SEM) out of 10 trials per day over an 11-day period, with day 11 being a session of post-choice baiting trials. The broken line denotes chance levels of performance (50% correct choices).

(B) Hippocampal-lesioned and *Gria1/3*$^{\Delta Fb}$ mice were unable to solve the spatial working memory, non-match to place (rewarded alternation) appetitively motivated T-maze task, with performance levels at near chance levels for the duration of the task in both groups. The control and sham-operated animals, however, were able to acquire the task after 5 blocks of training. In (A) and (B), the figure shows the mean correct choices made per block of 10 trials (±SEM). The broken line denotes chance levels of performance (50% correct choices). ***$p \leq 0.001$.

Furthermore, there was an effect of day for the control mice [$F(9, 270) = 19.32$; $p < 0.001$], *Gria1/3*$^{\Delta Fb}$ mice [$F(9,270) = 24.16$; $p < 0.001$] and sham-operated animals [$F(9,270) = 15.26$; $p < 0.001$] but not for the hippocampal-lesioned mice ($F < 1$; $p > 0.9$). Further investigation of the main effect of group using Newman-Keuls post-hoc comparisons revealed that the hippocampal-lesioned group was impaired compared to the other three groups ($p < 0.01$), and the sham animals were also different from the other two groups ($p < 0.01$).

Given our specific interest in the performance of the *Gria1/3*$^{\Delta Fb}$ mice, a separate ANOVA restricted to just the *Gria1/3*$^{\Delta Fb}$ mice and their control littermates was conducted and showed no effect of group [$F(1,15) = 2.41$; $p > 0.1$], a main effect of day [$F(9,135) = 37.15$; $p < 0.0001$] but no groups by days interaction [$F(9, 135) = 1.3$; $p > 0.2$], confirming that there was no deficit in the *Gria1/3*$^{\Delta Fb}$ mice when compared specifically to their control counterparts. The performance of mice did not change during the last block of trials when post-choice baiting was carried out, demonstrating that the mice were not solving the task by smelling the milk reward. A repeated-measures ANOVA of blocks 10 and 11 (the final block of training and the post-choice baiting block) revealed no effect of day, nor a genotype by day interaction (both $F < 1$; $p > 0.5$). In summary, unlike hippocampal-lesioned animals, *Gria1/3*$^{\Delta Fb}$ mice were able to learn a simple hippocampus-dependent spatial reference memory Y-maze task.

T-maze spatial working memory task

Next, we assessed spatial working memory performance using a non-matching to place rewarded alternation T-maze task, a task that is highly sensitive to both hippocampal damage and GluA1 deficiency.[27,59–62] In this task, hippocampal-lesioned and *Gria1/3*$^{\Delta Fb}$ mice were substantially impaired compared to the two control groups (Figure 4B). A two-way repeated measures ANOVA revealed a significant main effect of group [$F(3,30) = 27.27$; $p < 0.0001$], and also of block [$F(4, 120) = 22.29$; $p < 0.0001$], and a groups by blocks interaction [$F(12, 120) = 6.11$; $p < 0.001$]. Newman-Keuls post-hoc comparisons revealed no significant differences between the control and sham-lesioned animals, nor were there any differences between the *Gria1/3*$^{\Delta Fb}$ mice and hippocampal-lesioned animals. However, there were differences between the control and sham groups when compared to both *Gria1/3*$^{\Delta Fb}$ and hippocampal-lesioned groups ($p < 0.01$).

This spatial working memory deficit in the *Gria1/3*$^{\Delta Fb}$ mice was also evident in a test of spontaneous alternation conducted in the absence of appetitive rewards,[63,64] as part of the initial test battery performed (Table S1). Previous studies have shown that both hippocampal lesions and GluA1 deficiency also impair spontaneous alternation performance.[60,65]

Spatial reference memory in the radial maze

The lack of a spatial reference memory impairment in the *Gria1/3*$^{\Delta Fb}$ mice on the Y-maze was surprising. Therefore, we next assessed spatial reference memory using a 6-arm radial maze task. We have shown previously that spatial reference memory performance on the radial maze is dependent on the hippocampus but is unaffected in GluA1-deficient mice.[28] Mice were trained to discriminate between 3 always rewarded arms and 3 never rewarded arms, defined by the allocentric extramaze cues, thus increasing the mnemonic demands on the mice. Doors prevented mice from re-entering arms and thus from making working memory errors during this initial acquisition phase.[28] The control and sham mice were again easily able to acquire this task. However, the hippocampal-lesioned animals were significantly impaired during radial maze reference memory acquisition. The *Gria1/3*$^{\Delta Fb}$ mice acquired the task but at a slower rate than the control groups (Figure 5A). A two-way repeated-measures ANOVA revealed an effect of group {$F(3, 30) = 177.76$; $p < 0.0001$), an effect of block [$F(23, 690) = 38.2$; $p < 0.0001$], and a groups by blocks interaction [$F(69, 690) = 6.25$; $p < 0.0001$]. Simple main effects revealed an effect of block for controls [$F(23,690) = 13.32$; $p < 0.001$], *Gria1/3*$^{\Delta Fb}$ mice [$F(23,690) = 26.59$; $p < 0.001$] and sham-operated mice [$F(23,690) = 14.00$; $p < 0.001$], but not for the hippocampal-lesioned group ($F < 1$; $p > 0.2$). Again, a separate comparison was made between just the *Gria1/3*$^{\Delta Fb}$ mice and their control littermates. ANOVA revealed a significant main effect of group [$F(1,15) = 48.13$; $p < 0.0001$], an effect of block [$F(23,345) = 36.77$; $p < 0.0001$], and a groups by blocks interaction [$F(23,345) = 2.05$; $p < 0.005$]. Therefore, there was a substantial impairment in the *Gria1/3*$^{\Delta Fb}$ mice, although they did eventually manage to acquire the task to a level comparable with the controls.

Next, the working memory component of the task was introduced, and the mice were now allowed to re-enter arms they had already chosen on that trial. Only the *Gria1/3*$^{\Delta Fb}$ and control mice were tested in this phase of the experiment as a substantial reference memory impairment was already evident in the hippocampal-lesioned mice. Unsurprisingly, given the profound working memory deficit reported previously for *Gria1*$^{-/-}$ knockout mice,[28] the *Gria1/3*$^{\Delta Fb}$ mice were also dramatically impaired, making more spatial working memory (SWM) errors into the initially rewarded arms than controls [main effect of group ($F(1,15) = 213.45$; $p < 0.0001$) (Figure 5B). Notably, the *Gria1/3*$^{\Delta Fb}$ mice made substantially more spatial reference memory (SRM) errors during this phase of the task [main effect of group $F(1,15) = 55.59$; $p < 0.0001$] (Figure 5C), and also more working memory-incorrect errors whereby the re-entered a never-baited arm for a second time on a given trial [main effect of group ($F(1,15) = 22.11$; $p < 0.0001$] (Figure 5B). Thus, *Gria1/3*$^{\Delta Fb}$ mice resembled global *Gria1*$^{-/-}$ mice in displaying a substantial spatial working memory deficit in the radial maze.[62,66] However, *Gria1/3*$^{\Delta Fb}$ mice also showed a clear SRM deficit during acquisition on this task, which was not present in *Gria1*$^{-/-}$ knockout animals.

Spatial reference memory in the Morris water maze

Finally, we assessed hippocampus-dependent, spatial reference memory using the standard, fixed location, hidden escape platform version of the MWM task. It has been shown that performance on this task is unaffected in *Gria1*$^{-/-}$ knockout mice [e.g.,[26,27]], but is dependent on AMPAR/KARs in the hippocampus.[4]

In terms of escape latencies to find the platform during training, both control and sham-operated mice exhibited a gradual improvement across days, but neither hippocampal-lesioned mice nor *Gria1/3*$^{\Delta Fb}$ mice showed any signs of learning (Figure 6A). A two-way repeated-measures ANOVA revealed a significant main effect of group [$F(3,30) = 77.01$; $p < 0.001$], a main effect of day [$F(8,240) = 13.84$; $p < 0.001$], and a significant groups by days interaction [$F(24,305) = 5.18$; $p < 0.001$]. Post-hoc Newman-Keuls pairwise comparisons revealed significant differences (i) between the hippocampal-lesioned group and sham, control and *Gria1/3*$^{\Delta Fb}$ mice; (ii) between the *Gria1/3*$^{\Delta Fb}$ mice and both sham and control mice, and (iii) between sham and controls. Similar results were found for the pathlengths to the platform during acquisition (Figure 6B). A two-way repeated-measures ANOVA revealed a main effect of group [$F(3, 30) = 22.02$; $p < 0.001$], an effect of day [$F(8, 240) = 27.62$; $p < 0.001$] and a significant groups by days interaction [$F(24, 240) = 4.86$; $p < 0.001$]. Post-hoc Newman-Keuls comparisons revealed a significant difference (i) between the hippocampal-lesioned group and both the sham and control groups, but not between the lesioned and *Gria1/3*$^{\Delta Fb}$ mice, and (ii) between the *Gria1/3*$^{\Delta Fb}$ mice and both the sham and control mice.

Transfer tests (during which the platform was removed and the mice allowed to swim freely for 60 s) were used to assess spatial memory performance after 24 and 36 training trials (Figure 6C). In both of these probe tests, the sham and control mice searched preferentially in the training (Goal) quadrant (where the platform was normally located during the acquisition of the task), whereas neither the hippocampal-lesioned mice nor the *Gria1/3*$^{\Delta Fb}$ mice showed any such quadrant preference. ANOVA comparing the time spent in the training quadrant by the four groups revealed a significant main effect of group in both probe tests [Test 1 - ($F(3,30) = 4.89$; $p < 0.01$; Test 2 - ($F(3,30) = 5.96$; $p < 0.05$)]. Further analysis with post-hoc Newman-Keuls pairwise comparisons revealed significant differences in Probe Test 1 between controls and both the hippocampal-lesioned and *Gria1/3*$^{\Delta Fb}$ mice ($p < 0.05$). For Probe Test 2, there were significant differences between the sham group and both the *Gria1/3*$^{\Delta Fb}$ and hippocampal-lesioned mice ($p < 0.05$); and between the controls and both the *Gria1/3*$^{\Delta Fb}$ and hippocampal-lesioned mice ($p < 0.05$), but importantly, there were no differences between the *Gria1/3*$^{\Delta Fb}$ and hippocampal-lesioned mice ($p > 0.5$). Throughout the experiment, there was some evidence of floating behavior exhibited to various extents, which was most pronounced in the hippocampal-lesioned animals (mice with at least one incidence of floating - control 0 out of 7; shams 2 out of 7; *Gria1/3*$^{\Delta Fb}$ 2 out of 10; hippocampal-lesioned mice 8 out of 10). Thus, in contrast to single GluA1 and GluA3 knockout mice, *Gria1/3*$^{\Delta Fb}$ mice failed to learn the position of the submerged platform in the MWM, similar to hippocampal-lesioned mice.

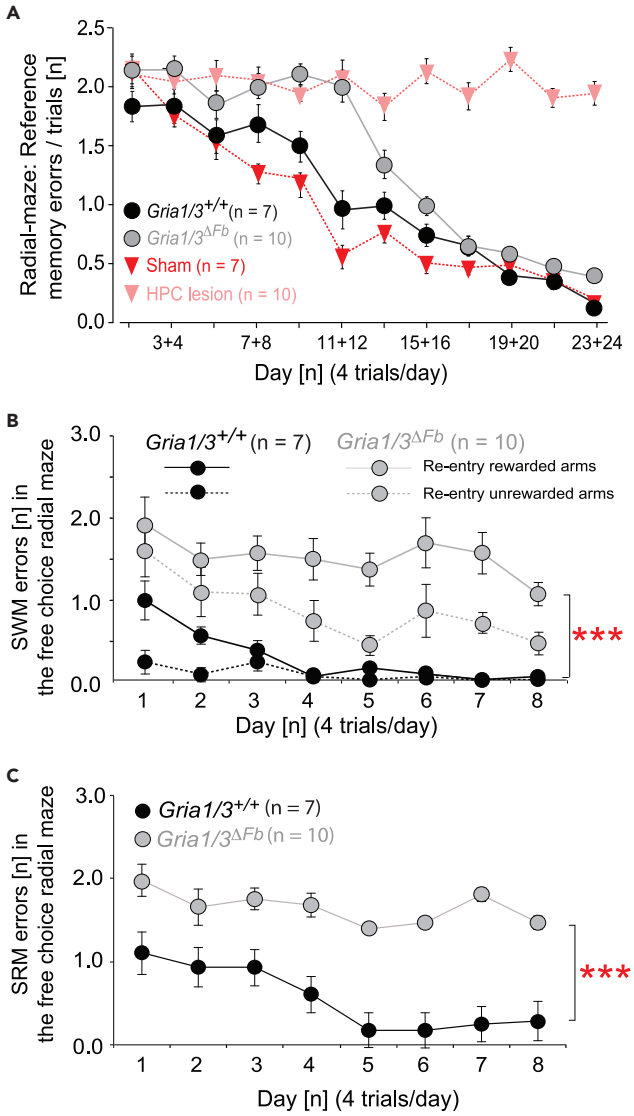

Figure 5. Spatial learning in the radial arm maze

(A) The *Gria1/3*$^{\Delta Fb}$ mice were impaired on the 3/6 radial maze reference memory task although they were eventually able to acquire the task. The hippocampal-lesioned animals showed high error rates throughout testing. The sham, control and *Gria1/3*$^{\Delta Fb}$ animals all displayed decreasing error rates, showing their ability to learn the task. The *Gria1/3*$^{\Delta Fb}$ animals, however, showed impairment in task acquisition.

(B) In the second phase of the radial maze task (simultaneous assessment of working and reference memory), *Gria1/3*$^{\Delta Fb}$ mice made significantly more repeat visits to previously baited arms and repeat visits into the never baited arms (i.e., spatial working memory (SWM) errors). In (A) and (B), the graph shows mean working memory errors per trial (±SEM).

(C) The results show a pronounced increase in the number of spatial reference memory errors (SRM) made per block in *Gria1/3*$^{\Delta Fb}$ mice during the second phase. *Gria1/3*$^{\Delta Fb}$ mice showed a significantly higher number of daily errors on this task than the control mice (±SEM). ***$p \leq 0.001$.

DISCUSSION

To assess the contribution of AMPAR subunits to hippocampus-dependent memory performance, we generated global and conditional knockout mice in which both the GluA1 and GluA3 subunits were ablated to enable comparison with previous studies analyzing the AMPAR single gene knockout mice[21,26,27][for review, see Gugustea and Jia (2021)[67]]. Global *Gria1/3*$^{-/-}$ knockout mice were viable under supportive conditions and exhibited no major histological or immunohistological cross-anomalies in the brain but showed severe developmental and basic behavioral impairments. This is reminiscent of the global *Gria2/3*$^{-/-}$ knockouts which displayed increased mortality and a gradual appearance of global abnormalities from 2 to 4 weeks after birth, including smaller body sizes, reduced locomotor activities, and severe tremors upon movement.[22] In contrast, conditional *Gria1/3*$^{\Delta Fb}$ mice were viable and amenable to further analysis.

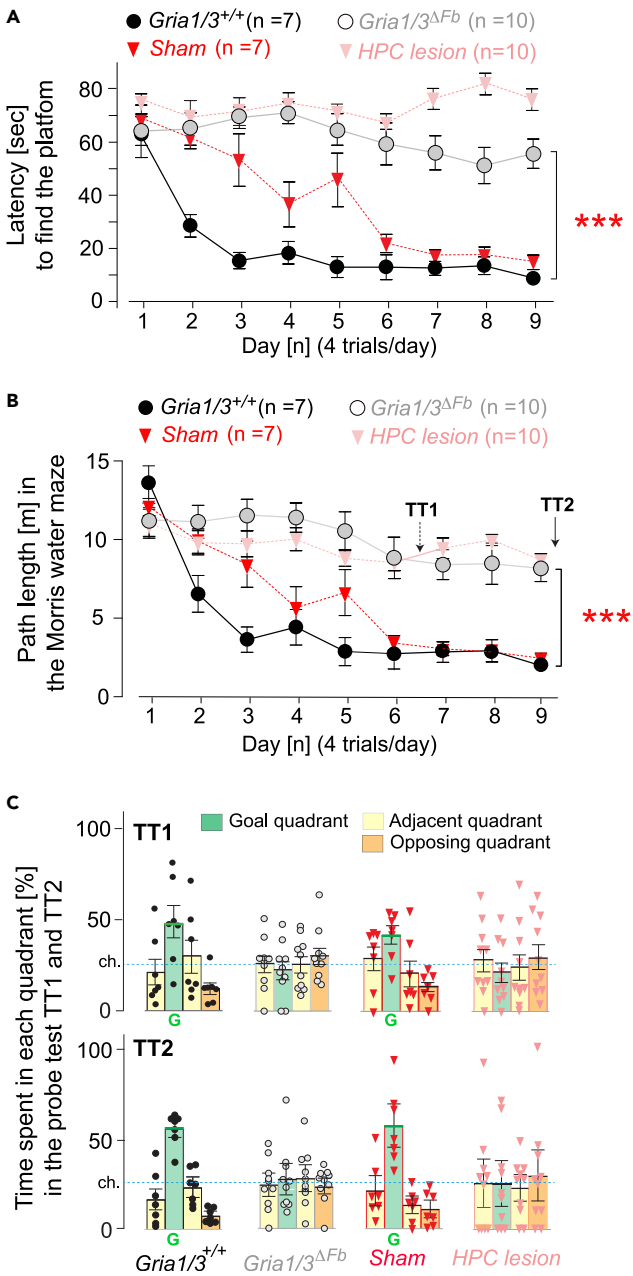

Figure 6. *Gria1/3*$^{\Delta Fb}$ and hippocampal-lesioned mice were unable to acquire the spatial reference memory Morris water maze task

(A) The control and sham mice showed decreasing latency to find the submerged platform but the *Gria1/3*$^{\Delta Fb}$ and hippocampal-lesioned mice showed no clear reduction in the latencies.

(B) The pathlength to reach the platform decreased across trials during the task, but the *Gria1/3*$^{\Delta Fb}$ and hippocampal-lesioned mice showed no clear reduction of the path lengths. The time points when the first and second transfer tests [(TT1) and (TT2)] given in Figure 6C were performed are indicated by arrows. For A aund B: The figure shows the mean latency and path length taken to reach the escape platform (±SEM).

(C) In both transfer tests (TT1 and TT2), the control and sham lesion animals spent significantly longer searching in the training (Goal) quadrant than in the adjacent or opposing quadrants. The hippocampal-lesioned and *Gria1/3*$^{\Delta Fb}$ mice showed no such spatial preference during either probe trials. The figure shows the mean percentage of time spent in each quadrant during the test (+SEM). The green bars summarize the time spent by the mice in the target quadrant, the yellow bars summarize the times spent in the adjacent left or right quadrant, and the orange bar summarizes the times spent in the opposite quadrants. The broken line denotes chance levels of performance during the probe test (25% in each quadrant of the pool). The experimental data on sham and hippocampal-lesioned mice are given in light gray since they were previously published [see supplementary information of Bannerman et al. 2012 [45]]. ***$p \leq 0.001$.

Changes in glutamate subunit receptor expression in *Gria1/3*$^{-/-}$ and *Gria1/3*$^{\Delta Fb}$ mice

Ablation of the *Gria1* and *Gria3* genes was verified by the reduced expression of the GluA1 and GluA3 subunits according to immunoblots on hippocampal extracts from the conditional *Gria1/3*$^{\Delta Fb}$ knockout mice. In addition, these immunohistochemical analyses of both *Gria1/3*$^{-/-}$ and *Gria1/3*$^{\Delta Fb}$ demonstrated a retention followed by a possible degradation of the GluA2 subunit in the cell body layer of the principal cells in the hippocampus. This may be explained by an assembly and/or trafficking deficit associated with the Q/R site-edited GluA2 homodimers or homotetramers that are not delivered to the cell membrane.[10–12] Surprisingly, the combined ablation of GluA1 and GluA3 in both the *Gria1/3*$^{-/-}$ and *Gria1/3*$^{\Delta Fb}$ mice was associated with an increase in hippocampal NMDAR subunits, which suggested the activation of compensatory mechanisms when the AMPAR population is reduced.

Fast synaptic transmission and synaptic plasticity are impaired in *Gria1/3*$^{\Delta Fb}$ mice

The simultaneous knockout of the GluA1 and GluA3 subunits could be demonstrated by the substantial reduction of synaptic CA1 AMPAR currents that was even more pronounced than the reduced CA1 currents described for *Gria2/3*$^{-/-}$[22,44] and *Gria1*$^{-}$*/2*$^{\Delta Fb}$ mice ["GluA3 only"[40]]. This result is in agreement with the observation that principal neurons expressing only the Q/R site-edited GluA2 show very little AMPAR currents.[41] By the pharmacological analysis of the EPSCs and EPSPs at CA3-to-CA1 synapses of *Gria1/3*$^{-/-}$ mice, compensatory NMDA and non-NMDA components could be detected, which were not observed in *Gria1*$^{-/-}$ or *Gria3*$^{-/-}$ mice. However, the tetanic stimulation of CA3-to-CA1 synapses could not induce field LTP, which is also absent in GluA1$^{-/-}$ mice, but is GluA1 independent in young animals.[26,46] Instead, a kind of LTD could be observed in two week old *Gria1/3*$^{-/-}$ mice.

It is conceivable that in the absence of GluA1-mediated transmission, other mechanisms for the induction of the CA3-to-CA1 synaptic plasticity can support hippocampus-dependent spatial learning (see also Bannerman et al., 2012; 2014[45,68]). The pairing and Theta-burst LTP protocols were able to activate such mechanisms in *Gria1*$^{-/-}$ and *Gria1*$^{-/-}$*/2*$^{\Delta Fb}$ mice as evidenced by the long-term potentiation at CA1 synapses of the respective genotypes.[35,36,40,46] Even in the absence of all AMPARs at hippocampal synapses, the long-term enhancement of synaptic transmission at CA3-to-CA1 synapses was obtained by these protocols.[69]

Thus, after more than 30 years of research with different LTP protocols [see for example Nicoll (2017)[70]] and many AMPAR knockout mice, it still remains to be worked out whether, and which form or forms of, experimentally induced synaptic plasticity are relevant for hippocampus-dependent long-term spatial learning.[67] Plasticity mechanisms that could be recruited in *Gria1/3*$^{\Delta Fb}$ mice might include the potentiation of presynaptic release[71] or the observed upregulation of NMDAR expression that leads to NMDAR-dependent LTD, for example.[72] It is also described that Arc expression might trigger a homeostatic form of synaptic plasticity by binding inactive CaMKIIβ to produce a relative potentiation at CaMKII-activated synapses.[73,74]

Furthermore, structural plasticity, i.e., the stabilization of new spines that relies on NMDAR activation[75] and CaMKII,[76] may be independent of AMPAR subunit composition or even independent of the presence of AMPARs, since knocking out all AMPAR subunits does not affect spine density at CA1 neurons.[41] The types of learning that require multiple repetitions may depend less on LTP and more on the creation of new connections.

It could be that *Gria1/3*$^{\Delta Fb}$ and *Gria1*$^{-/-}$*/2*$^{\Delta Fb}$ mice can form memories in the Y-maze task through structural plasticity, independently of AMPARs, particularly considering that the formation of GluA3 homomers, as present in *Gria1*$^{-/-}$*/2*$^{\Delta Fb}$ CA1 neurons, is energetically unfavorable.[48]

Impaired hippocampus-dependent spatial memory performance in *Gria1/3*$^{\Delta Fb}$ mice

In contrast to the obligatory role of GluA1-containing AMPAR in spatial short-term memory,[28,77,78] a redundancy of function exists with respect to the involvement of different AMPAR subunits in long-term spatial memory performance. In the Morris water maze (MWM), *Gria1/3*$^{\Delta Fb}$ mice showed profound long-term memory deficits, in marked contrast to the normal MWM learning previously seen in both the single *Gria1*$^{-/-}$ and *Gria3*$^{-/-}$ knockout mice. Thus, in long-term spatial memory, the GluA3 subunit can compensate for the absence of GluA1 and vice versa. However, when AMPAR synaptic transmission is no longer detectable in dorsal hippocampal excitatory neurons, other mechanisms may emerge, including for example in the ventral hippocampus, but these may only be sufficient for some simple forms of spatial learning.

In our study, the *Gria1/3*$^{\Delta Fb}$ mice could still learn the hippocampus-dependent spatial reference memory in the Y-maze task but were unable to solve the MWM and the radial arm maze that is regarded as a more complex version of the three arm Y-maze. This argues against a simple sensorimotor or motivational account of the radial maze impairment in the *Gria1/3*$^{\Delta Fb}$ mice, and suggests that deficits become apparent in these mice as the memory demands increase. This is potentially important given the evidence of a mild motoric impairment in these animals (e.g., static rods tests) and their reduced muscle strength that could conceivably impact behavioral performance in these memory tasks. However, it is also worth noting that the *Gria1/3*$^{\Delta Fb}$ mice were hyperactive in a 2 h beam test for spontaneous locomotor activity, resembling mice with hippocampal lesions and *Gria1*$^{-/-}$ mice,[31,79–81] arguing against a poverty of movement in these animals.

The spatial memory deficit that we see in *Gria1/3*$^{\Delta Fb}$ mice is less severe compared to our hippocampal-lesioned animals that were analyzed side by side. This may indicate that the traditional postsynaptic AMPAR- and NMDAR-mediated synaptic plasticity and transmission at CA3-to-CA1 excitatory dorsal hippocampal synapses is not a strict requirement for memory performance in simpler spatial tasks in mice. In adult *Gria1/2*$^{\Delta Fb}$ and *Gria1/3*$^{\Delta Fb}$ mice, residual homomers of the GluA3 or GluA2 subunits, respectively are unlikely to support basic synaptic transmission as detailed in the introduction.

NMDAR, KARs, presynaptic components or structural plasticity are more likely to provide activity-dependent modulation of the synaptic transmission within the hippocampal circuits. Alternatively, the interneuron network might be adapted to the reduced excitatory transmission system, or the increased NMDAR density might facilitate experience-dependent neuroplasticity as noticed in pharmacological studies in rats and patients with psychiatric disorders.[82,83] Furthermore, some residual AMPAR activity, including for example in the ventral hippocampus, where the transgenic CaMKII promoter is less active[62] might compensate for spatial memory functions in the absence of a functional dorsal hippocampus although the ventral hippocampus is not normally associated with spatial memory.[84,85] It is also worth pointing out that our genetically modified mice do not allow us to differentiate between a deficit in learning and an impairment in memory recall [see Riedel et al. 1999[4]].

Based on our earlier observations that GluA1-deficient mice are models of impaired synaptic plasticity relevant to schizophrenia,[29,77,86,87] and that GluA2(Q/R) editing-deficient mice with drastically increased numbers of Ca^{2+}-permeable AMPAR are associated with epilepsy,[88,89] the subsequent genetic analyses of neurological and neuropsychological patients have shown that GluA1, 2 and 3 AMPAR subunit mutations can all be associated with such disorders [e.g.,[90–93]]. From this perspective, it is of particular interest to describe the learning and memory processes that are disrupted, and those which are spared in the presence of defective AMPAR signaling. This might provide important hints for the treatment and therapy of diseases with severe AMPAR signaling impairment.

Limitations of the study

The present study did not explore in detail compensatory mechanism(s) that are activated when AMPARs are depleted in excitatory neurons and did not investigate the etiology and molecular mechanisms underlying the decreased levels of GluA2 in the GluA1/3 knockout mice (e.g., reduced expression, reduced secretion, or increased degradation). Additionally, other protocols for the induction of cellular plasticity were not pursued and were only mentioned in reference to other publications that used the floxed Gria1, 2 and 3 mice.[33,39,41,94] In future studies, it would be of interest to analyze potential alterations that may occur in other brain regions involved in memory (e.g., the medial entorhinal cortex), as well as changes in the balance of excitation/inhibition, theta/gamma oscillations, or activity of place cells. Furthermore, it is important to acknowledge that while the knockout approach employed in this study was highly informative and elucidative, it has the limitation of not enabling the differentiation between deficits in learning and impairments in memory recall.

STAR★METHODS

Detailed methods are provided in the online version of this paper and include the following:

- KEY RESOURCES TABLE
- RESOURCE AVAILABILITY
  - Lead contact
  - Materials availability
  - Data and code availability
- EXPERIMENTAL MODEL AND STUDY PARTICIPANT DETAILS
  - Experimental animals
- METHOD DETAILS
  - Immunohistochemistry
  - Immunoblots
  - Single cell recordings
  - Field LTP recordings
  - Preliminary behavioral analysis of Gria1/3$^{\Delta Fb}$ mice
  - Extended behavioral analysis of Gria1/3$^{\Delta Fb}$ mice
  - Spontaneous alternation
  - Memory tests
- QUANTIFICATION AND STATISTICAL ANALYSIS

SUPPLEMENTAL INFORMATION

Supplemental information can be found online at https://doi.org/10.1016/j.isci.2023.108116.

ACKNOWLEDGMENTS

We thank Annette Herold for her expert technical assistance and genotyping of the mice. Our sincere thanks go to our colleagues Øivind Hvalby, Per Andersen and Peter H. Seeburg, who were involved in these experiments. Parts of this work were released in poster presentations at meetings of the Society for Neuroscience: Celekil et al. (2005) and Hasenkamp et al., (2006); SfN Posters 395.19 and 53.12, respectively, and in the PhD thesis from TB at Heidelberg University (2002) and the master's thesis from AT at Oxford University (2007). This study was supported in part by a grant from the Wellcome trust SRF 074385/Z/04/Z to DB and by the German Research Council to RS (SP602/1, SFB636/A4 and SFB1134/B01). RS receives support from the Ingeborg Ständer Foundation. VJ was supported by (EU-Grant QLRT-1999-01022 LTP

expression). AR is supported by Russian Science Foundation grant 22-15-00293. AE received support from a postdoctoral fellowship from Fritz Thyssen Stiftung and a NARSAD young investigator grant from the Brain and Behavior Research Foundation (BBRF). The funders had no role in the study design, data collection and analysis, decision to publish, or preparation of the article.

AUTHOR CONTRIBUTIONS

TB and RS generated and molecularly analyzed the mouse lines. VJ and AR performed and analyzed the electrophysiological experiments in acute brain slices. AE, AT, CP, JNPR, and DB designed, performed, and analyzed the behavioral experiments. IB, TB and CP performed the histological analysis and immunoblots. AE, RS and DB analyzed the data and prepared the figures. AE and DB performed the statistical analysis. RS, AE, IB, and DB wrote the article.

DECLARATION OF INTERESTS

The authors declare no competing interests.

INCLUSION AND DIVERSITY

We support inclusive, diverse, and equitable conduct of research. One or more of the authors of this paper self-identifies as living with a disability.

Received: October 25, 2022
Revised: July 1, 2023
Accepted: September 29, 2023
Published: October 1, 2023

REFERENCES

1. Henley, J.M., and Wilkinson, K.A. (2016). Synaptic AMPA receptor composition in development, plasticity and disease. Nat. Rev. Neurosci. *17*, 337–350. https://doi.org/10.1038/nrn.2016.37.
2. Malinow, R. (2003). AMPA receptor trafficking and long-term potentiation. Philos. Trans. R. Soc. Lond. B Biol. Sci. *358*, 707–714. https://doi.org/10.1098/rstb.2002.1233.
3. Larsen, A.M., and Bunch, L. (2011). Medicinal chemistry of competitive kainate receptor antagonists. ACS Chem. Neurosci. *2*, 60–74. https://doi.org/10.1021/cn1001039.
4. Riedel, G., Micheau, J., Lam, A.G., Roloff, E.L., Martin, S.J., Bridge, H., de Hoz, L., Poeschel, B., McCulloch, J., and Morris, R.G. (1999). Reversible neural inactivation reveals hippocampal participation in several memory processes. Nat. Neurosci. *2*, 898–905. https://doi.org/10.1038/13202.
5. Keinänen, K., Wisden, W., Sommer, B., Werner, P., Herb, A., Verdoorn, T.A., Sakmann, B., and Seeburg, P.H. (1990). A family of AMPA-selective glutamate receptors. Science *249*, 556–560. https://doi.org/10.1126/science.2166337.
6. Monyer, H., Seeburg, P.H., and Wisden, W. (1991). Glutamate-operated channels: developmentally early and mature forms arise by alternative splicing. Neuron *6*, 799–810. https://doi.org/10.1016/0896-6273(91)90176-z.
7. Wisden, W., and Seeburg, P.H. (1993). A complex mosaic of high-affinity kainate receptors in rat brain. J. Neurosci. *13*, 3582–3598. https://doi.org/10.1523/JNEUROSCI.13-08-03582.1993.
8. Gan, Q., Salussolia, C.L., and Wollmuth, L.P. (2015). Assembly of AMPA receptors: mechanisms and regulation. J. Physiol. *593*, 39–48. https://doi.org/10.1113/jphysiol.2014.273755.
9. Schwenk, J., Boudkkazi, S., Kocylowski, M.K., Brechet, A., Zolles, G., Bus, T., Costa, K., Kollewe, A., Jordan, J., Bank, J., et al. (2019). An ER Assembly Line of AMPA-Receptors Controls Excitatory Neurotransmission and Its Plasticity. Neuron *104*, 680–692.e9. https://doi.org/10.1016/j.neuron.2019.08.033.
10. Greger, I.H., Khatri, L., and Ziff, E.B. (2002). RNA editing at arg607 controls AMPA receptor exit from the endoplasmic reticulum. Neuron *34*, 759–772. https://doi.org/10.1016/s0896-6273(02)00693-1.
11. Araki, Y., Lin, D.T., and Huganir, R.L. (2010). Plasma membrane insertion of the AMPA receptor GluA2 subunit is regulated by NSF binding and Q/R editing of the ion pore. Proc. Natl. Acad. Sci. USA *107*, 11080–11085. https://doi.org/10.1073/pnas.1006584107.
12. Coleman, S.K., Hou, Y., Willibald, M., Semenov, A., Möykkynen, T., and Keinänen, K. (2016). Aggregation Limits Surface Expression of Homomeric GluA3 Receptors. J. Biol. Chem. *291*, 8784–8794. https://doi.org/10.1074/jbc.M115.689125.
13. Sommer, B., Köhler, M., Sprengel, R., and Seeburg, P.H. (1991). RNA editing in brain controls a determinant of ion flow in glutamate-gated channels. Cell *67*, 11–19. https://doi.org/10.1016/0092-8674(91)90568-j.
14. Zhu, J.J., Esteban, J.A., Hayashi, Y., and Malinow, R. (2000). Postnatal synaptic potentiation: delivery of GluR4-containing AMPA receptors by spontaneous activity. Nat. Neurosci. *3*, 1098–1106. https://doi.org/10.1038/80614.
15. Pelkey, K.A., Barksdale, E., Craig, M.T., Yuan, X., Sukumaran, M., Vargish, G.A., Mitchell, R.M., Wyeth, M.S., Petralia, R.S., Chittajallu, R., et al. (2016). Pentraxins Coordinate Excitatory Synapse Maturation and Circuit Integration of Parvalbumin Interneurons. Neuron *90*, 661. https://doi.org/10.1016/j.neuron.2016.04.024.
16. Luchkina, N.V., Coleman, S.K., Huupponen, J., Cai, C., Kivistö, A., Taira, T., Keinänen, K., and Lauri, S.E. (2017). Molecular mechanisms controlling synaptic recruitment of GluA4 subunit-containing AMPA-receptors critical for functional maturation of CA1 glutamatergic synapses. Neuropharmacology *112*, 46–56. https://doi.org/10.1016/j.neuropharm.2016.04.049.
17. Fuchs, E.C., Zivkovic, A.R., Cunningham, M.O., Middleton, S., Lebeau, F.E.N., Bannerman, D.M., Rozov, A., Whittington, M.A., Traub, R.D., Rawlins, J.N.P., and Monyer, H. (2007). Recruitment of parvalbumin-positive interneurons determines hippocampal function and associated behavior. Neuron *53*, 591–604. https://doi.org/10.1016/j.neuron.2007.01.031.
18. Sagata, N., Iwaki, A., Aramaki, T., Takao, K., Kura, S., Tsuzuki, T., Kawakami, R., Ito, I., Kitamura, T., Sugiyama, H., et al. (2010). Comprehensive behavioural study of GluR4 knockout mice: implication in cognitive function. Gene Brain Behav. *9*, 899–909. https://doi.org/10.1111/j.1601-183X.2010.00629.x.
19. Adamczyk, A., Mejias, R., Takamiya, K., Yocum, J., Krasnova, I.N., Calderon, J., Cadet, J.L., Huganir, R.L., Pletnikov, M.V., and Wang, T. (2012). GluA3-deficiency in mice is associated with increased social and aggressive behavior and elevated dopamine in striatum. Behav. Brain Res. *229*, 265–272. https://doi.org/10.1016/j.bbr.2012.01.007.
20. García-Hernández, S., Abe, M., Sakimura, K., and Rubio, M.E. (2017). Impaired auditory processing and altered structure of the endbulb of Held synapse in mice lacking the GluA3 subunit of AMPA receptors. Hear.

Res. *344*, 284–294. https://doi.org/10.1016/j.heares.2016.12.006.

21. Sanchis-Segura, C., Borchardt, T., Vengeliene, V., Zghoul, T., Bachteler, D., Gass, P., Sprengel, R., and Spanagel, R. (2006). Involvement of the AMPA receptor GluR-C subunit in alcohol-seeking behavior and relapse. J. Neurosci. *26*, 1231–1238. https://doi.org/10.1523/JNEUROSCI.4237-05.2006.
22. Meng, Y., Zhang, Y., and Jia, Z. (2003). Synaptic transmission and plasticity in the absence of AMPA glutamate receptor GluR2 and GluR3. Neuron *39*, 163–176. https://doi.org/10.1016/s0896-6273(03)00368-4.
23. Italia, M., Ferrari, E., Di Luca, M., and Gardoni, F. (2021). GluA3-containing AMPA receptors: From physiology to synaptic dysfunction in brain disorders. Neurobiol. Dis. *161*, 105539. https://doi.org/10.1016/j.nbd.2021.105539.
24. Jia, Z., Agopyan, N., Miu, P., Xiong, Z., Henderson, J., Gerlai, R., Taverna, F.A., Velumian, A., MacDonald, J., Carlen, P., et al. (1996). Enhanced LTP in mice deficient in the AMPA receptor GluR2. Neuron *17*, 945–956. https://doi.org/10.1016/s0896-6273(00)80225-1.
25. Wenthold, R.J., Petralia, R.S., Blahos J, I.I., Niedzielski, A.S., and Niedzielski, A.S. (1996). Evidence for multiple AMPA receptor complexes in hippocampal CA1/CA2 neurons. J. Neurosci. *16*, 1982–1989. https://doi.org/10.1523/JNEUROSCI.16-06-01982.
26. Zamanillo, D., Sprengel, R., Hvalby, O., Jensen, V., Burnashev, N., Rozov, A., Kaiser, K.M., Köster, H.J., Borchardt, T., Worley, P., et al. (1999). Importance of AMPA receptors for hippocampal synaptic plasticity but not for spatial learning. Science *284*, 1805–1811. https://doi.org/10.1126/science.284.5421.1805.
27. Reisel, D., Bannerman, D.M., Schmitt, W.B., Deacon, R.M.J., Flint, J., Borchardt, T., Seeburg, P.H., and Rawlins, J.N.P. (2002). Spatial memory dissociations in mice lacking GluR1. Nat. Neurosci. *5*, 868–873. https://doi.org/10.1038/nn910.
28. Schmitt, W.B., Deacon, R.M.J., Seeburg, P.H., Rawlins, J.N.P., and Bannerman, D.M. (2003). A within-subjects, within-task demonstration of intact spatial reference memory and impaired spatial working memory in glutamate receptor-A-deficient mice. J. Neurosci. *23*, 3953–3959. https://doi.org/10.1523/JNEUROSCI.23-09-03953.
29. Fitzgerald, P.J., Barkus, C., Feyder, M., Wiedholz, L.M., Chen, Y.C., Karlsson, R.M., Machado-Vieira, R., Graybeal, C., Sharp, T., Zarate, C., et al. (2010). Does gene deletion of AMPA GluA1 phenocopy features of schizoaffective disorder? Neurobiol. Dis. *40*, 608–621. https://doi.org/10.1016/j.nbd.2010.08.005.
30. Sanderson, D.J., Lee, A., Sprengel, R., Seeburg, P.H., Harrison, P.J., and Bannerman, D.M. (2017). Altered balance of excitatory and inhibitory learning in a genetically modified mouse model of glutamatergic dysfunction relevant to schizophrenia. Sci. Rep. *7*, 1765. https://doi.org/10.1038/s41598-017-01925-8.
31. Wiedholz, L.M., Owens, W.A., Horton, R.E., Feyder, M., Karlsson, R.M., Hefner, K., Sprengel, R., Celikel, T., Daws, L.C., and Holmes, A. (2008). Mice lacking the AMPA GluR1 receptor exhibit striatal hyperdopaminergia and 'schizophrenia-related' behaviors. Mol. Psychiatr. *13*, 631–640. https://doi.org/10.1038/sj.mp.4002056.
32. Panayi, M.C., Boerner, T., Jahans-Price, T., Huber, A., Sprengel, R., Gilmour, G., Sanderson, D.J., Harrison, P.J., Walton, M.E., and Bannerman, D.M. (2023). Glutamatergic dysfunction leads to a hyperdopaminergic phenotype through deficits in short-term habituation: a mechanism for aberrant salience. Mol. Psychiatr. *28*, 579–587. https://doi.org/10.1038/s41380-022-01861-8.
33. Freudenberg, F., Marx, V., Seeburg, P.H., Sprengel, R., and Celikel, T. (2013). Circuit mechanisms of GluA1-dependent spatial working memory. Hippocampus *23*, 1359–1366. https://doi.org/10.1002/hipo.22184.
34. Kilonzo, K., Strahnen, D., Prex, V., Gems, J., van der Veen, B., Kapanaiah, S.K.T., Murthy, B.K.B., Schulz, S., Sprengel, R., Bannerman, D., and Kätzel, D. (2022). Distinct contributions of GluA1-containing AMPA receptors of different hippocampal subfields to salience processing, memory and impulse control. Transl. Psychiatry *12*, 102. https://doi.org/10.1038/s41398-022-01863-8.
35. Frey, M.C., Sprengel, R., and Nevian, T. (2009). Activity pattern-dependent long-term potentiation in neocortex and hippocampus of GluA1 (GluR-A) subunit-deficient mice. J. Neurosci. *29*, 5587–5596. https://doi.org/10.1523/JNEUROSCI.5314-08.2009.
36. Hoffman, D.A., Sprengel, R., and Sakmann, B. (2002). Molecular dissection of hippocampal theta-burst pairing potentiation. Proc. Natl. Acad. Sci. USA *99*, 7740–7745. https://doi.org/10.1073/pnas.092157999.
37. Romberg, C., Raffel, J., Martin, L., Sprengel, R., Seeburg, P.H., Rawlins, J.N.P., Bannerman, D.M., and Paulsen, O. (2009). Induction and expression of GluA1 (GluR-A)-independent LTP in the hippocampus. Eur. J. Neurosci. *29*, 1141–1152. https://doi.org/10.1111/j.1460-9568.2009.06677.x.
38. Andrásfalvy, B.K., Smith, M.A., Borchardt, T., Sprengel, R., and Magee, J.C. (2003). Impaired regulation of synaptic strength in hippocampal neurons from GluR1-deficient mice. J. Physiol. *552*, 35–45. https://doi.org/10.1113/jphysiol.2003.045575.
39. Shimshek, D.R., Jensen, V., Celikel, T., Geng, Y., Schupp, B., Bus, T., Mack, V., Marx, V., Hvalby, Ø., Seeburg, P.H., and Sprengel, R. (2006). Forebrain-specific glutamate receptor B deletion impairs spatial memory but not hippocampal field long-term potentiation. J. Neurosci. *26*, 8428–8440. https://doi.org/10.1523/JNEUROSCI.5410-05.2006.
40. Shimshek, D.R., Bus, T., Schupp, B., Jensen, V., Marx, V., Layer, L.E., Köhr, G., and Sprengel, R. (2017). Different Forms of AMPA Receptor Mediated LTP and Their Correlation to the Spatial Working Memory Formation. Front. Mol. Neurosci. *10*, 214. https://doi.org/10.3389/fnmol.2017.00214.
41. Lu, W., Shi, Y., Jackson, A.C., Bjorgan, K., During, M.J., Sprengel, R., Seeburg, P.H., and Nicoll, R.A. (2009). Subunit composition of synaptic AMPA receptors revealed by a single-cell genetic approach. Neuron *62*, 254–268. https://doi.org/10.1016/j.neuron.2009.02.027.
42. Bannerman, D.M., Borchardt, T., Jensen, V., Rozov, A., Haj-Yasein, N.N., Burnashev, N., Zamanillo, D., Bus, T., Grube, I., Adelmann, G., et al. (2018). Somatic Accumulation of GluA1-AMPA Receptors Leads to Selective Cognitive Impairments in Mice. Front. Mol. Neurosci. *11*, 199. https://doi.org/10.3389/fnmol.2018.00199.
43. Catania, M.V., Bellomo, M., Giuffrida, R., Giuffrida, R., Stella, A.M., and Albanese, V. (1998). AMPA receptor subunits are differentially expressed in parvalbumin- and calretinin-positive neurons of the rat hippocampus. Eur. J. Neurosci. *10*, 3479–3490. https://doi.org/10.1046/j.1460-9568.1998.00356.x.
44. Renner, M.C., Albers, E.H., Gutierrez-Castellanos, N., Reinders, N.R., van Huijstee, A.N., Xiong, H., Lodder, T.R., and Kessels, H.W. (2017). Synaptic plasticity through activation of GluA3-containing AMPA-receptors. Elife *6*, e25462. https://doi.org/10.7554/eLife.25462.
45. Bannerman, D.M., Bus, T., Taylor, A., Sanderson, D.J., Schwarz, I., Jensen, V., Hvalby, Ø., Rawlins, J.N.P., Seeburg, P.H., and Sprengel, R. (2012). Dissecting spatial knowledge from spatial choice by hippocampal NMDA receptor deletion. Nat. Neurosci. *15*, 1153–1159. https://doi.org/10.1038/nn.3166.
46. Jensen, V., Kaiser, K.M.M., Borchardt, T., Adelmann, G., Rozov, A., Burnashev, N., Brix, C., Frotscher, M., Andersen, P., Hvalby, Ø., et al. (2003). A juvenile form of postsynaptic hippocampal long-term potentiation in mice deficient for the AMPA receptor subunit GluR-A. J. Physiol. *553*, 843–856. https://doi.org/10.1113/jphysiol.2003.053637.
47. Lu, W., Khatri, L., and Ziff, E.B. (2014). Trafficking of alpha-amino-3-hydroxy-5-methyl-4-isoxazolepropionic acid receptor (AMPA) receptor subunit GluA2 from the endoplasmic reticulum is stimulated by a complex containing Ca2+/calmodulin-activated kinase II (CaMKII) and PICK1 protein and by release of Ca2+ from internal stores. J. Biol. Chem. *289*, 19218–19230. https://doi.org/10.1074/jbc.M113.511246.
48. Rossmann, M., Sukumaran, M., Penn, A.C., Veprintsev, D.B., Babu, M.M., and Greger, I.H. (2011). Subunit-selective N-terminal domain associations organize the formation of AMPA receptor heteromers. EMBO J. *30*, 959–971. https://doi.org/10.1038/emboj.2011.16.
49. Greger, I.H., Khatri, L., Kong, X., and Ziff, E.B. (2003). AMPA receptor tetramerization is mediated by Q/R editing. Neuron *40*, 763–774. https://doi.org/10.1016/s0896-6273(03)00668-8.
50. Gutierrez-Castellanos, N., Da Silva-Matos, C.M., Zhou, K., Canto, C.B., Renner, M.C., Koene, L.M.C., Ozyildirim, O., Sprengel, R., Kessels, H.W., and De Zeeuw, C.I. (2017). Motor Learning Requires Purkinje Cell Synaptic Potentiation through Activation of AMPA-Receptor Subunit GluA3. Neuron *93*, 409–424. https://doi.org/10.1016/j.neuron.2016.11.046.
51. Fukaya, M., Kato, A., Lovett, C., Tonegawa, S., and Watanabe, M. (2003). Retention of NMDA receptor NR2 subunits in the lumen of endoplasmic reticulum in targeted NR1 knockout mice. Proc. Natl. Acad. Sci. USA *100*, 4855–4860. https://doi.org/10.1073/pnas.0830996100.

52. Mack, V., Burnashev, N., Kaiser, K.M., Rozov, A., Jensen, V., Hvalby, O., Seeburg, P.H., Sakmann, B., and Sprengel, R. (2001). Conditional restoration of hippocampal synaptic potentiation in Glur-A-deficient mice. Science *292*, 2501–2504. https://doi.org/10.1126/science.1059365.
53. Mayford, M., Bach, M.E., Huang, Y.Y., Wang, L., Hawkins, R.D., and Kandel, E.R. (1996). Control of memory formation through regulated expression of a CaMKII transgene. Science *274*, 1678–1683. https://doi.org/10.1126/science.274.5293.1678.
54. Minichiello, L., Korte, M., Wolfer, D., Kühn, R., Unsicker, K., Cestari, V., Rossi-Arnaud, C., Lipp, H.P., Bonhoeffer, T., and Klein, R. (1999). Essential role for TrkB receptors in hippocampus-mediated learning. Neuron *24*, 401–414. https://doi.org/10.1016/s0896-6273(00)80853-3.
55. Feyder, M., Wiedholz, L., Sprengel, R., and Holmes, A. (2007). Impaired associative fear learning in mice with complete loss or haploinsufficiency of AMPA GluR1 receptors. Front. Behav. Neurosci. *1*, 4. https://doi.org/10.3389/neuro.08.004.2007.
56. Humeau, Y., Reisel, D., Johnson, A.W., Borchardt, T., Jensen, V., Gebhardt, C., Bosch, V., Gass, P., Bannerman, D.M., Good, M.A., et al. (2007). A pathway-specific function for different AMPA receptor subunits in amygdala long-term potentiation and fear conditioning. J. Neurosci. *27*, 10947–10956. https://doi.org/10.1523/JNEUROSCI.2603-07.2007.
57. Morris, R.G., Garrud, P., Rawlins, J.N., and O'Keefe, J. (1982). Place navigation impaired in rats with hippocampal lesions. Nature *297*, 681–683. https://doi.org/10.1038/297681a0.
58. O'Keefe, J., and Nadel, L. (1978). The Hippocampus as a Cognitive Map (Oxford: Clarendon Press).
59. Rawlins, J.N., and Olton, D.S. (1982). The septo-hippocampal system and cognitive mapping. Behav. Brain Res. *5*, 331–358. https://doi.org/10.1016/0166-4328(82)90039-0.
60. Deacon, R.M.J., Bannerman, D.M., Kirby, B.P., Croucher, A., and Rawlins, J.N.P. (2002). Effects of cytotoxic hippocampal lesions in mice on a cognitive test battery. Behav. Brain Res. *133*, 57–68. https://doi.org/10.1016/s0166-4328(01)00451-x.
61. Gerlai, R. (1998). A new continuous alternation task in T-maze detects hippocampal dysfunction in mice. A strain comparison and lesion study. Behav. Brain Res. *95*, 91–101. https://doi.org/10.1016/s0166-4328(97)00214-3.
62. Schmitt, W.B., Sprengel, R., Mack, V., Draft, R.W., Seeburg, P.H., Deacon, R.M.J., Rawlins, J.N.P., and Bannerman, D.M. (2005). Restoration of spatial working memory by genetic rescue of GluR-A-deficient mice. Nat. Neurosci. *8*, 270–272. https://doi.org/10.1038/nn1412.
63. Bannerman, D.M., Yee, B.K., Good, M.A., Heupel, M.J., Iversen, S.D., and Rawlins, J.N. (1999). Double dissociation of function within the hippocampus: a comparison of dorsal, ventral, and complete hippocampal cytotoxic lesions. Behav. Neurosci. *113*, 1170–1188. https://doi.org/10.1037//0735-7044.113.6.1170.
64. Deacon, R.M.J., and Rawlins, J.N.P. (2006). T-maze alternation in the rodent. Nat. Protoc. *1*, 7–12. https://doi.org/10.1038/nprot.2006.2.
65. Bannerman, D.M., Deacon, R.M.J., Brady, S., Bruce, A., Sprengel, R., Seeburg, P.H., and Rawlins, J.N.P. (2004). A comparison of GluR-A-deficient and wild-type mice on a test battery assessing sensorimotor, affective, and cognitive behaviors. Behav. Neurosci. *118*, 643–647. https://doi.org/10.1037/0735-7044.118.3.643.
66. Schmitt, W.B., Arianpour, R., Deacon, R.M.J., Seeburg, P.H., Sprengel, R., Rawlins, J.N.P., and Bannerman, D.M. (2004). The role of hippocampal glutamate receptor-A-dependent synaptic plasticity in conditional learning: the importance of spatiotemporal discontiguity. J. Neurosci. *24*, 7277–7282. https://doi.org/10.1523/JNEUROSCI.1093-04.2004.
67. Gugustea, R., and Jia, Z. (2021). Genetic manipulations of AMPA glutamate receptors in hippocampal synaptic plasticity. Neuropharmacology *194*, 108630. https://doi.org/10.1016/j.neuropharm.2021.108630.
68. Bannerman, D.M., Sprengel, R., Sanderson, D.J., McHugh, S.B., Rawlins, J.N.P., Monyer, H., and Seeburg, P.H. (2014). Hippocampal synaptic plasticity, spatial memory and anxiety. Nat. Rev. Neurosci. *15*, 181–192. https://doi.org/10.1038/nrn3677.
69. Granger, A.J., Shi, Y., Lu, W., Cerpas, M., and Nicoll, R.A. (2013). LTP requires a reserve pool of glutamate receptors independent of subunit type. Nature *493*, 495–500. https://doi.org/10.1038/nature11775.
70. Nicoll, R.A. (2017). A Brief History of Long-Term Potentiation. Neuron *93*, 281–290. https://doi.org/10.1016/j.neuron.2016.12.015.
71. Chipman, P.H., Fetter, R.D., Panzera, L.C., Bergerson, S.J., Karmelic, D., Yokoyama, S., Hoppa, M.B., and Davis, G.W. (2022). NMDAR-dependent presynaptic homeostasis in adult hippocampus: Synapse growth and cross-modal inhibitory plasticity. Neuron *110*, 3302–3317.e7. https://doi.org/10.1016/j.neuron.2022.08.014.
72. Granger, A.J., and Nicoll, R.A. (2014). LTD expression is independent of glutamate receptor subtype. Front. Synaptic Neurosci. *6*, 15. https://doi.org/10.3389/fnsyn.2014.00015.
73. Okuno, H., Akashi, K., Ishii, Y., Yagishita-Kyo, N., Suzuki, K., Nonaka, M., Kawashima, T., Fujii, H., Takemoto-Kimura, S., Abe, M., et al. (2012). Inverse synaptic tagging of inactive synapses via dynamic interaction of Arc/Arg3.1 with CaMKIIbeta. Cell *149*, 886–898. https://doi.org/10.1016/j.cell.2012.02.062.
74. Rial Verde, E.M., Lee-Osbourne, J., Worley, P.F., Malinow, R., and Cline, H.T. (2006). Increased expression of the immediate-early gene arc/arg3.1 reduces AMPA receptor-mediated synaptic transmission. Neuron *52*, 461–474. https://doi.org/10.1016/j.neuron.2006.09.031.
75. Alvarez, V.A., Ridenour, D.A., and Sabatini, B.L. (2007). Distinct structural and ionotropic roles of NMDA receptors in controlling spine and synapse stability. J. Neurosci. *27*, 7365–7376. https://doi.org/10.1523/JNEUROSCI.0956-07.2007.
76. Kim, K., Lakhanpal, G., Lu, H.E., Khan, M., Suzuki, A., Hayashi, M.K., Narayanan, R., Luyben, T.T., Matsuda, T., Nagai, T., et al. (2015). A Temporary Gating of Actin Remodeling during Synaptic Plasticity Consists of the Interplay between the Kinase and Structural Functions of CaMKII. Neuron *87*, 813–826. https://doi.org/10.1016/j.neuron.2015.07.023.
77. Barkus, C., Sanderson, D.J., Rawlins, J.N.P., Walton, M.E., Harrison, P.J., and Bannerman, D.M. (2014). What causes aberrant salience in schizophrenia? A role for impaired short-term habituation and the GRIA1 (GluA1) AMPA receptor subunit. Mol. Psychiatr. *19*, 1060–1070. https://doi.org/10.1038/mp.2014.91.
78. Sanderson, D.J., and Bannerman, D.M. (2012). The role of habituation in hippocampus-dependent spatial working memory tasks: evidence from GluA1 AMPA receptor subunit knockout mice. Hippocampus *22*, 981–994. https://doi.org/10.1002/hipo.20896.
79. Praag, H.v., Dreyfus, C.F., and Black, I.B. (1994). Dissociation of motor hyperactivity and spatial memory deficits by selective hippocampal lesions in the neonatal rat. J. Cognit. Neurosci. *6*, 321–331. https://doi.org/10.1162/jocn.1994.6.4.321.
80. Bannerman, D.M., Lemaire, M., Beggs, S., Rawlins, J.N., and Iversen, S.D. (2001). Cytotoxic lesions of the hippocampus increase social investigation but do not impair social-recognition memory. Exp. Brain Res. *138*, 100–109. https://doi.org/10.1007/s002210100687.
81. Aitta-Aho, T., Maksimovic, M., Dahl, K., Sprengel, R., and Korpi, E.R. (2019). Attenuation of Novelty-Induced Hyperactivity of Gria1-/- Mice by Cannabidiol and Hippocampal Inhibitory Chemogenetics. Front. Pharmacol. *10*, 309. https://doi.org/10.3389/fphar.2019.00309.
82. Forsyth, J.K., Bachman, P., Mathalon, D.H., Roach, B.J., and Asarnow, R.F. (2015). Augmenting NMDA receptor signaling boosts experience-dependent neuroplasticity in the adult human brain. Proc. Natl. Acad. Sci. USA *112*, 15331–15336. https://doi.org/10.1073/pnas.1509262112.
83. Zhou, X., Cai, G., Mao, S., Xu, D., Xu, X., Zhang, R., and Yao, Z. (2020). Modulating NMDA receptors to treat MK-801-induced schizophrenic cognition deficit: effects of clozapine combining with PQQ treatment and possible mechanisms of action. BMC Psychiatr. *20*, 106. https://doi.org/10.1186/s12888-020-02509-z.
84. Bannerman, D.M., Rawlins, J.N.P., McHugh, S.B., Deacon, R.M.J., Yee, B.K., Bast, T., Zhang, W.N., Pothuizen, H.H.J., and Feldon, J. (2004). Regional dissociations within the hippocampus–memory and anxiety. Neurosci. Biobehav. Rev. *28*, 273–283. https://doi.org/10.1016/j.neubiorev.2004.03.004.
85. de Hoz, L., Knox, J., and Morris, R.G.M. (2003). Longitudinal axis of the hippocampus: both septal and temporal poles of the hippocampus support water maze spatial learning depending on the training protocol. Hippocampus *13*, 587–603. https://doi.org/10.1002/hipo.10079.
86. Bygrave, A.M., Jahans-Price, T., Wolff, A.R., Sprengel, R., Kullmann, D.M., Bannerman, D.M., and Kätzel, D. (2019). Hippocampal-prefrontal coherence mediates working memory and selective attention at distinct frequency bands and provides a causal link between schizophrenia and its risk gene

GRIA1. Transl. Psychiatry *9*, 142. https://doi.org/10.1038/s41398-019-0471-0.

87. Inta, D., Monyer, H., Sprengel, R., Meyer-Lindenberg, A., and Gass, P. (2010). Mice with genetically altered glutamate receptors as models of schizophrenia: a comprehensive review. Neurosci. Biobehav. Rev. *34*, 285–294. https://doi.org/10.1016/j.neubiorev.2009.07.010.
88. Brusa, R., Zimmermann, F., Koh, D.S., Feldmeyer, D., Gass, P., Seeburg, P.H., and Sprengel, R. (1995). Early-onset epilepsy and postnatal lethality associated with an editing-deficient GluR-B allele in mice. Science *270*, 1677–1680. https://doi.org/10.1126/science.270.5242.1677.
89. Feldmeyer, D., Kask, K., Brusa, R., Kornau, H.C., Kolhekar, R., Rozov, A., Burnashev, N., Jensen, V., Hvalby, O., Sprengel, R., and Seeburg, P.H. (1999). Neurological dysfunctions in mice expressing different levels of the Q/R site-unedited AMPAR subunit GluR-B. Nat. Neurosci. *2*, 57–64. https://doi.org/10.1038/4561.
90. Ismail, V., Zachariassen, L.G., Godwin, A., Sahakian, M., Ellard, S., Stals, K.L., Baple, E., Brown, K.T., Foulds, N., Wheway, G., et al. (2022). Identification and functional evaluation of GRIA1 missense and truncation variants in individuals with ID: An emerging neurodevelopmental syndrome. Am. J. Hum. Genet. *109*, 1217–1241. https://doi.org/10.1016/j.ajhg.2022.05.009.
91. Peng, S.X., Pei, J., Rinaldi, B., Chen, J., Ge, Y.H., Jia, M., Wang, J., Delahaye-Duriez, A., Sun, J.H., Zang, Y.Y., et al. (2022). Dysfunction of AMPA receptor GluA3 is associated with aggressive behavior in human. Mol. Psychiatr. *27*, 4092–4102. https://doi.org/10.1038/s41380-022-01659-8.
92. Salpietro, V., Dixon, C.L., Guo, H., Bello, O.D., Vandrovcova, J., Efthymiou, S., Maroofian, R., Heimer, G., Burglen, L., Valence, S., et al. (2019). AMPA receptor GluA2 subunit defects are a cause of neurodevelopmental disorders. Nat. Commun. *10*, 3094. https://doi.org/10.1038/s41467-019-10910-w.
93. Singh, T., Poterba, T., Curtis, D., Akil, H., Al Eissa, M., Barchas, J.D., Bass, N., Bigdeli, T.B., Breen, G., Bromet, E.J., et al. (2022). Rare coding variants in ten genes confer substantial risk for schizophrenia. Nature *604*, 509–516. https://doi.org/10.1038/s41586-022-04556-w.
94. Engblom, D., Bilbao, A., Sanchis-Segura, C., Dahan, L., Perreau-Lenz, S., Balland, B., Parkitna, J.R., Luján, R., Halbout, B., Mameli, M., et al. (2008). Glutamate receptors on dopamine neurons control the persistence of cocaine seeking. Neuron *59*, 497–508. https://doi.org/10.1016/j.neuron.2008.07.010.
95. Schönig, K., Schwenk, F., Rajewsky, K., and Bujard, H. (2002). Stringent doxycycline dependent control of CRE recombinase *in vivo*. Nucleic Acids Res. *30*, e134. https://doi.org/10.1093/nar/gnf134.
96. Laemmli, U.K. (1970). Cleavage of structural proteins during the assembly of the head of bacteriophage T4. Nature *227*, 680–685. https://doi.org/10.1038/227680a0.
97. Bertocchi, I., Eltokhi, A., Rozov, A., Chi, V.N., Jensen, V., Bus, T., Pawlak, V., Serafino, M., Sonntag, H., Yang, B., et al. (2021). Voltage-independent GluN2A-type NMDA receptor Ca(2+) signaling promotes audiogenic seizures, attentional and cognitive deficits in mice. Commun. Biol. *4*, 59. https://doi.org/10.1038/s42003-020-01538-4.
98. Jarvik, M.E., and Kopp, R. (1967). An improved one-trial passive avoidance learning situation. Psychol. Rep. *21*, 221–224. https://doi.org/10.2466/pr0.1967.21.1.221.
99. Deacon, R.M.J., Croucher, A., and Rawlins, J.N.P. (2002). Hippocampal cytotoxic lesion effects on species-typical behaviours in mice. Behav. Brain Res. *132*, 203–213. https://doi.org/10.1016/s0166-4328(01)00401-6.
100. Deacon, R.M.J., Penny, C., and Rawlins, J.N.P. (2003). Effects of medial prefrontal cortex cytotoxic lesions in mice. Behav. Brain Res. *139*, 139–155.
101. Deacon, R.M.J. (2006). Burrowing in rodents: a sensitive method for detecting behavioral dysfunction. Nat. Protoc. *1*, 118–121.
102. Slotnick, B.M., and Nigrosh, B.J. (1975). Maternal behavior of mice with cingulate cortical, amygdala, or septal lesions. J. Comp. Physiol. Psychol. *88*, 118–127.
103. Deacon, R.M.J. (2006). Assessing nest building in mice. Nat. Protoc. *1*, 1117–1119.
104. Burns, L.H., Annett, L., Kelley, A.E., Everitt, B.J., and Robbins, T.W. (1996). Effects of lesions to amygdala, ventral subiculum, medial prefrontal cortex, and nucleus accumbens on the reaction to novelty: implication for limbic-striatal interactions. Behav. Neurosci. *110*, 60–73.
105. McHugh, S.B., Deacon, R.M.J., Rawlins, J.N.P., and Bannerman, D.M. (2004). Amygdala and ventral hippocampus contribute differentially to mechanisms of fear and anxiety. Behav. Neurosci. *118*, 63–78.
106. Crawley, J.N. (1981). Neuropharmacologic specificity of a simple animal model for the behavioral actions of benzodiazepines. Pharmacol. Biochem. Behav. *15*, 695–699. https://doi.org/10.1016/0091-3057(81)90007-1.
107. Bourin, M., and Hascoët, M. (2003). The mouse light/dark box test. Eur. J. Pharmacol. *463*, 55–65.
108. Deacon, R.M.J., Brook, R.C., Meyer, D., Haeckel, O., Ashcroft, F.M., Miki, T., Seino, S., and Liss, B. (2006). Behavioral phenotyping of mice lacking the K ATP channel subunit Kir6.2. Physiol. Behav. *87*, 723–733.
109. Cunningham, C., Deacon, R.M.J., Chan, K., Boche, D., Rawlins, J.N.P., and Perry, V.H. (2005). Neuropathologically distinct prion strains give rise to similar temporal profiles of behavioral deficits. Neurobiol. Dis. *18*, 258–269.
110. Guenther, K., Deacon, R.M., Perry, V.H., and Rawlins, J.N. (2001). Early behavioural changes in scrapie-affected mice and the influence of dapsone. Eur. J. Neurosci. *14*, 401–409.
111. Contet, C., Rawlins, J.N., and Deacon, R.M. (2001). A comparison of 129S2/SvHsd and C57BL/6JOlaHsd mice on a test battery assessing sensorimotor, affective and cognitive behaviours: implications for the study of genetically modified mice. Behav. Brain Res. *124*, 33–46. https://doi.org/10.1016/s0166-4328(01)00231-5.
112. Betmouni, S., Clements, J., and Perry, V.H. (1999). Vacuolation in murine prion disease: an informative artifact. Curr. Biol. *9*, R677–R679.

STAR★METHODS

KEY RESOURCES TABLE

REAGENT or RESOURCE	SOURCE	IDENTIFIER
Antibodies		
Rabbit polyclonal anti-Glutamate Receptor 1 (anti-GluA1)	Millipore	Cat# AB1504
Rabbit polyclonal anti-Glutamate Receptor 2 (anti-GluA2)	Millipore Sigma	Cat# AB1768
Mouse monoclonal anti-Glutamate Receptor 3 (anti-GluA3)	Thermo Fisher	Cat# 32-0400
Rabbit polyclonal anti-Glutamate Receptor 4 (anti-GluA4)	Millipore Sigma	Cat# AB1508
Mouse monoclonal anti-NMDAR1antibody (anti-GluN1)	BD Pharmingen	Cat# 556308
Rabbit polyclonal anti-NMDAR2A antibody (anti-GluN2A)	Upstate	Cat# 06-313
Rabbit polyclonal anti-NMDAR2B antibody (anti-GluN2B)	Fisher Scientific	Cat# AB1557
Mouse monoclonal anti-β-Actin (anti-β-Actin)	Millipore Sigma	Cat# Ac15
Mouse monoclonal anti-NeuN (anti NeuN)	Millipore Sigma	Cat# MAB377
Mouse monoiclonal anti-MAP2 (anti MAP2)	Millipore Sigma	Cat# M4403
Rabbit polyclonal anti-Glial Fibrillary Protein (anti-GFAP)	Agilent Dako	Cat# Z0334
Mouse monoclomnal anti-βIIITubulin (anti-Tubulin)	Millipore Sigma	Cat# MAB1637
Mouse monoclonal anti-Synaptophysin (anti-Synaptophsin)	Millipore Sigma	Cat# MAB5258-20UG
Mouse monoclamal anti-α-CaMKII	Millipore Sigma	Cat# MAB3119
Rabbit polyclonal Cre recombinase (anti-Cre)	Thermo Fisher	Cat# PA5-32244
Peroxidase-conjugated AffiniPure Goat anti-Rabbit IgG[H+L]	Dianova	Cat# 111-035-144
Peroxidase-conjugated AffiniPure Goat Anti-Mouse IgG[H+L]	Dianova	Cat# 115-035-003
Chemicals, peptides, and recombinant proteins		
EUKITT® classic Mounting Media for Microscopy	Orsatec/Kindler	N/A
cOmplete™, EDTA-free Protease Inhibitor Cocktail	Millipore Sigma	Cat# 11873580001
ECL Plus Western Blotting Substrate	Amersham Bioscience	N/A
(2,3-dihydroxy-6-nitro-7-sulfamoyl-benzo(F)quinoxaline) NBQX disodium salt	Tocris	Cat# 1044
(D-2-amino-5-phosphonovalerate) D-APV	Tocris	Cat# 0106
(1-(4-aminophenyl)-4-methyl-7,8-methylenedioxy-5H-2,3-benzodiazepine hydrochlorid) GYKI 52466 dihydrochloride	Tocris	Cat# 1454
(2,3-dihydroxy-6-nitro-7-sulfamoyl-benzo(F)quinoxaline) NBQX disodium salt	Tocris	Cat# 1044
Critical commercial assays		
BCA Protein Assay Kit	Thermo Fisher	Cat# 23225
Experimental models: Organisms/strains		
C57BL/6N Mice (WT, controls) WT controls & hippocampoal lesioned mice	Charles river/DE Harlan/UK Bicester	RRID MGI:2159965
B6N-*Gria1*$^{tm1Rsp/J}$ (*Gria1*$^{-/-}$)	The Jackson laboratory	RRID:IMSR_JAX:019011
B6N-*Gria1*^{tm2RspJ} (*Gria1*$^{f/f}$)	The Jackson laboratory	RRID:IMSR_JAX:019012
B6.Cg-*Tg*$^{(Camk2a-tTA)1Mmay/DboJ}$	The Jackson laboratory	RRID:IMSR_JAX:007004

(*Continued on next page*)

Continued

REAGENT or RESOURCE	SOURCE	IDENTIFIER
B6.129-*Gria3*$^{tm1Rsp/Kctt}$ (*Gria3*$^{f/f}$)	European Mouse Mutant Archive (EMMA	RRID:IMSR_EM:09215
B6.Cg-*Tg*$^{(tetO\text{-}cre)LC1Bjd/BJdCnrm}$ (*Tg*$^{(tetO\text{-}Cre)LC}$)	The Jackson laboratory & European Mouse Mutant Archive (EMMA	RRID:IMSR_EM:00753
Others		
normal diet food pellets	Lasvendi GMBH	LASQCdiet Rod18, auto
LAS3000 Luminescent Imager Analyser	FUJI	https://wie-tec.de/
Zeiss Axioimager	Zeiss	https://www.zeiss.com
Axiovision Imaging system	Zeiss	RRID: SCR_002677
Software and algorithms		
ImageJ 1.52a	NIH	RRID:SCR:003070
Microsoft Excel	Microsoft Corporation	RRID:SCR_016137
GraphPad Prism 9	GraphPad Software	RRID:SCR_002798
Adobe Illustrator	Adobe Systems	RRID: SCR_010279
Adobe Photoshop	Adobe Systems	RRID: SCR_014199
AxioVision		RRID: SCR_002677

RESOURCE AVAILABILITY

Lead contact

Further information and requests for resources and reagents should be directed to and will be fulfilled by the Lead Contact, Rolf Sprengel sprengel@mr.mpg.de.

Materials availability

This study did not generate new unique reagents.

Data and code availability

- Data reported in this paper will be shared by the lead contact upon request.
- This paper does not report original code.
- Any additional information required to reanalyze the data reported in this paper is available from the lead contact upon request.

EXPERIMENTAL MODEL AND STUDY PARTICIPANT DETAILS

Experimental animals

Generation of the Gria1/3$^{-/-}$ mice

For the generation of *Gria1/3*$^{-/-}$ mice, matings between *Gria1*$^{-/-}$[26] and *Gria3*$^{-/-}$ mice[21] were employed. First, *Gria1*$^{-/-}$ mice were crossed with homozygous *Gria3*$^{-/-}$ mice to produce *Gria1*$^{+/-}$/*Gria3*$^{+/-}$ female mice and hemizygous *Gria1*$^{+/-}$/*Gria3*$^{Y/-}$ males. In the second step, these two genotypes were used together with *Gria1*$^{-/-}$ to generate *Gria1*$^{-/-}$/*Gria3*$^{+/-}$ and *Gria1*$^{-/-}$/*Gria3*$^{Y/-}$ mice. In a third step, *Gria1*$^{+/-}$/*Gria3*$^{+/-}$ and *Gria1*$^{-/-}$/*Gria3*$^{+/-}$ females and *Gria1*$^{+/-}$/*Gria3*$^{Y/-}$ males were used to generate the experimental cohorts [*Gria1/3*$^{-/-}$ = *Gria1*$^{-/-}$/*Gria3*$^{-/-}$, *Gria1*$^{-/-}$/*Gria3*$^{Y/-}$; Controls: males *Gria1/3*$^{+/+}$, female *Gria1/3*$^{+/+}$ and *Gria1*$^{+/+}$/*3*$^{+/-}$ mice. Genotyping for the *Gria1* and *Gria3* loci was done as described in Zamanillo et al.[26] and Sanchis-Segura et al.[21] respectively. Between P0 and P2, offspring were separated from their mothers and transferred to NMRI foster mothers. Furthermore, after weaning, between P19 and P21, offspring were provided with additional high caloric, wet food pellets. *Gria1/3*$^{+/-}$ female offspring and littermates homozygous for one of the knockout alleles were comparable to single heterozygous or control littermates in growth rate and body robustness. However, *Gria1/3*$^{-/-}$ females and *Gria1/3*$^{Y/-}$ males differed significantly from their littermates. Both could be recognized by late eyelid opening, delayed growth, smaller body size, and lower body weight. Due to their physical weakness, the adolescent *Gria1/3*$^{-/-}$ and *Gria1/3*$^{Y/-}$ genotypes had difficulty reaching the food shelf and the water bottle

in the cage lid, but could be kept viable in their home cages with NMRI foster mothers and wet, rich food pellets in the bedding. Under those conditions, *Gria1/3*$^{-/-}$ and *Gria3*$^{Y/-}$ animals reached a normal life expectancy.

Generation of Gria1/3$^{\Delta Fb}$ mice

Gria1$^{f/f}$ and *Gria3*$^{f/f}$ were used in several previous studies [see main text]. *Gria1/3*$^{\Delta Fb}$ mice were generated by mating double-positive *Gria1*^{ff}/*3*^{ff} mice with the *Tg*$^{(tetO\text{-}Cre)LC1}$mouse line,[95] which contains a Cre recombinase transgene (Cre) regulated by the $tetO_7$ transactivator operator sequence that can be activated by a tetracycline/VP16 transactivator (tA) transgene, under the control of a promoter fragment from the αCaMKII gene; *Tg*$^{Camk2a\text{-}tTA}$.[53] For the generation of the *Gria1/3*$^{\Delta Fb}$ and control cohorts, *Gria1*^{ff}/*3*^{ff}/*Tg*$^{(tetO\text{-}cre)LC1}$ were crossed with *Gria1*^{ff}/*3*^{ff}/*Tg*$^{Camk2a\text{-}tTA}$ mice. Transgenic littermates that lack one or both transgenes were used as controls. Genotyping was done by PCR of tail-biopsies with the following primer sets. For *Gria1* alleles; primers MH60: 5′-CAC TCA CAG CAA TGA AGC AGG-3′ and 3int3′: 5′-CTG CCT GGG TAA AGT GAC TTG G-3′; (250bp *Gria1*^{f} allele, 220bp WT allele); for *Gria3*^{f} alleles; primers RC2: 5′-CCA ATG TTG TGC TTT AGC CTT TGC-3′ and RC3: 5′-GGT ATA TCT TCC CAG CCC CAA G-3′ (300bp *Gria1*^{f} allele, 270bp WT allele). For the transgene *Tg*$^{(tetO\text{-}cre)LC1}$; sense luc1: 5′-TTA CAG ATG CAC ATA TCG AGG-3′; antisense luc2: 5′-TAA CCC AGT AGA TCC AGA GG-3′ (500bp) and for *Tg*$^{Camk2a\text{-}tTA}$, tTA multi1: 5′-GGA CGA GCT CCA CTT AGA CG-3′ and tTA multi2: 5′-AGG GCA TCG GGT AAA CAT CTG-3′. Alternative genotyping protocols are available for all mouse lines at the host of the respective mouse repository. The presence of the *Gria3* gene on the X Chromosome facilitated mating. All mouse lines used were backcrossed for several generations in C57BL/6N background. We did not observe any influence of sex in the mating or basic behavior in our study. A detailed comparative analysis was not performed.

Ethical statement

Animal experiments at the Max Planck Institute for Medical Research in Heidelberg were performed according to the institutional guidelines of the Max Planck Society and the 'Interfakultäre Biomedizinische Forschungseinrichtung' (IBF) animal core facility of the Heidelberg University. Genetic manipulations of mice were licensed by the Governmental Council Karlsruhe, Germany: Generation of mice (35-9185.81/G-4/02); mouse behavior (35-9185.81/G-71/10; 35-9185.81/G-171/10). Animals used for molecular, histological and electrophysiological experiments were recorded under the protocols MPI/T-6/06 and 15/08. *Ex vivo* LTP experiments were conducted according to the Norwegian Animal Welfare Act and the European Union's Directive 86/609/EEC. Behavioral experiments in the UK were conducted in accordance with the United Kingdom Animals Scientific Procedures Act (1986), under the project license number PPL 30/2561 of the U.K Home Office.

METHOD DETAILS

Immunohistochemistry

Mice were deeply anesthetized with halothane, followed by intracardial perfusion with PBS and 4% PFA in PBS. Brains were postfixed overnight, embedded in 2% agarose in PBS and cut either coronal or sagittal into 40–70 μm thick sections on a vibratome (Leica VT 1000S, Leica). For DAB immunostaining, slices were permeabilized for 30 min in Day1-buffer (0.3% Triton X-100, 2% BSA in PBS). After 3 washes in PBS, endogenous peroxidase activity was blocked with 1% H_2O_2 in PBS for 10 min. After 3 washes with PBS, slices were blocked in 8% normal goat serum in Day1-buffer for 1 h. Primary antibody incubation was done overnight in Day1-buffer at 4°C with slide shaking. The next day, slices were washed twice with Day2-buffer (1:3 diluted Day1-buffer with PBS) and secondary antibodies (1:600 in Day2-buffer) and were incubated for 2 hr. After one wash with Day2-buffer and two washes with PBS, slices were incubated with DAB-solution (0.4 mg DAB, 0.3% H_2O_2 in 20 mM Tris·Cl pH 7.6). The reaction was stopped by 2 washes in PBS and a final wash in 20 mM Tris·Cl pH 7.6. Slices were air-dried overnight, dipped into xylol and embedded in EUKITT. Antibodies were used for Cre-recombinase (rabbit polyclonal, 1:3000), GluA1 (anti-GluR-A; rabbit polyclonal, 1:200), GluA2 (anti-GluR-B; rabbit polyclonal, 1:25). Slides were imaged with Zeiss Axioimager M1 brightfield microscope with the software AxioVision version 4.6 (Axiocision system). Objectives 5x Zeiss EC PlanNeofluar dry, 0.16 NA and 10x Zeiss EC Plan-Neofluar dry, 0.45 NA were used mainly. For Figure S3, the following antibodies were used for immunohistochemical studies according to the supplier's instructions: anti-NeuN anti-MAP2, anti-GFAP), anti-βIIITubulin, anti-Synaptophysin, anti-αCaMKII). Secondary antibodies were Peroxidase-conjugated AffiniPure Goat Anti-Rabbit IgG[H+L] and Peroxidase-conjugated AffiniPure Goat Anti-Mouse IgG[H+L]; see KRT.

Immunoblots

Mice were anesthetized with isoflurane and decapitated. Total brains were isolated and hippocampi were prepared. Hippocampal protein samples were prepared using a Dounce homogenizer on ice in 25 mM HEPES pH 7.4 including a protease inhibitor Cocktail. After centrifugation at 2000 rpm for 5 min at 4°C to remove cell debris and nuclei, protein concentration was determined via BCA-Assay (Pierce). Eight μg of protein were separated via 7.5% SDS-PAGE,[96] and blotted onto nitrocellulose membranes (PA-85 Schleicher&Schuell) by wet transfer. After blocking the membranes with 8% dry milk powder in PBS-T (0.05% Tween 20 in PBS) for 2–3 hr, primary antibody incubation was done for 3 hr at RT with slide shaking. After 4 additional washes for 10 min in PBS-T, peroxidase-conjugated secondary antibodies were applied at 1:20000 dilutions in PBS-T for 45 min. After 4 additional washes with PBS-T, blots were developed with ECL+Plus on autoradiographic films and scanned by a CCD-camera at 600 dpi (LAS300, Fujifilm) for different time points of exposure. The following primary antibodies were used for Western blot studies: β-actin (mouse monoclonal, 1:20000), GluA1 (GluR-A; rabbit polyclonal, 1:2000), GluA2 (GluR-B; mouse monoclonal, 1:500), GluA3 (GluR-C; mouse monoclonal, 1:300), GluA4 (GluR-D; rabbit polyclonal, 1:250), GluN1 (NR1; mouse monoclonal, 1:500), GluN2A (NR2A; rabbit polyclonal, 1:250), GluN2B (NR2B; rabbit polyclonal, 1:250). *Quantification*: Signal intensities of individual immune-labeled

proteins of the CCD immunoblot images were quantified by ImageJ (NIH) and normalized to intensities of β-actin bands, which served as an internal control for the samples analyzed.

Single cell recordings

Transverse hippocampal 300 μm slices were prepared from the brains of control and *Gria1/3*$^{-/-}$ mice at P14 and P42. The slicing chamber contained an oxygenated ice-cold artificial cerebrospinal fluid (ACSF) containing (in mM): NaCl, 125; $NaHCO_3$, 25; KCl, 2.5; NaH_2PO_4, 1.25; $MgCl_2$, 1; $CaCl_2$, 2; and D-glucose, 25; bubbled with 95% O_2 and 5% CO_2. Slices were incubated for 30 min at 35°C before being stored at room temperature. During experiments, slices were continuously perfused with the same ACSF. Patch electrodes were pulled from hard borosilicate capillary glass (Sutter Instruments flaming/brown micropipette puller). Electrodes were filled with a solution consisting of (in mM): Cs-gluconate, 144; CsCl, 4; HEPES, 10; MgATP, 4; MgGTP, 0.3; phosphocreatine, 10 (pH 7.3 with CsOH). CA1 pyramidal cells were visually identified using IR-video microscopy. Whole-cell recordings from these neurons were taken at room temperature (23–25°C) in voltage-clamp mode using a HEKA EPC-7 amplifier (List Elektronik) with a sampling rate of 100 μs and filtered at 3 kHz. Spontaneous EPSCs in CA1 pyramidal neurons were recorded in voltage-clamp mode in hippocampal brain slices at a holding potential of -70 mV in the presence of 1 mM Mg^{2+}. The AMPA/NMDA current ratios were measured in Mg^{2+}-free ACSF. AMPA- and NMDA-mediated EPSCs were pharmacologically isolated by sequential bath application of D-APV (200 μM; 2-amino-5-phosphonovaleric acid; Tocis) and NBQX (10 μM; 6-cyano-7-nitroquinoxaline-2,3-dione; Tocis), respectively. First, the compound AMPAR and NMDAR-mediated current were recorded in Mg^{2+}-free ASCF. After collecting at least 100 sweeps, the AMPA-mediated component was blocked by the application of NBQX. Then, additional 100 sweeps of the NMDA-mediated currents were collected. The AMPA-mediated component was then obtained by subtracting the averaged NMDA-mediated currents from the averaged compound responses. The AMPA/NMDA ratio was calculated by dividing averaged amplitude of AMPAR EPSCs by the amplitude of NMDAR EPSCs.[97] In a separate set of experiments, identity of remaining fast AMPAR/KAR-meditated component in *Gria1/3*$^{-/-}$ mice was tested by sensitivity to the GYKI 52466 (50 μM; 1-(4-aminophenyl)-4-methyl-7,8-methylenedioxy-5H-2,3-benzodiazepine hydrochlorid, Tocis).

Field LTP recordings

Field EPSPs were recorded in CA1 of hippocampal slices prepared from mice sacrificed with halothane. Brain slices (400 μm thick) were maintained in an interface chamber [for details see Beertocchi et al., 2021.[97] Orthodromic synaptic stimulation (50μs < 300 μA, 0.2 Hz) in CA1 was delivered alternately through two tungsten electrodes to activate synapses in the apical (*str. radiatum*) and basal (*str. oriens*) dendrites. Extracellular potentials were monitored by similarly placed glass electrodes filled with extracellular solution. After obtaining stable synaptic responses in both pathways for at least 10 min, one pathway (e.g. *str. oriens*) was tetanized (100 Hz, 1 sec), and the other (e.g. *str. radiatum*) served as a control pathway. To standardize the tetanization strength, we set the tetanic stimulation strength in response to a single tetanic shock at an intensity just above the threshold for the generation of a population spike. We assessed synaptic efficacy by measuring the slope of the fEPSP in the middle third of its rising phase. Six consecutive responses (1 min) were averaged and normalized to the mean value recorded 4–7 min before the tetanic stimulation.[26,46] Our analyses revealed that the increased response after tetanization was achieved at a similar value in the *str. oriens* and *str. radiatum* synapses. In slices from adult control littermates, the response increase was on average 1.2505 for the *rad./oriens* and 1.3329 for the *oriens/rad.* arrangements (t-test/P_{value} = 0.422878). For adult *Gria1/3*$^{\Delta Fb}$, the values were 1.0251 and 1.075571 (P=0.48241), and for hippocampal slices from *Gria1/3*$^{-/-}$, the values were 1.0867 and 0.885 (P=0.021295). Based on our results from control littermates and *Gria1/3*$^{\Delta Fb}$ mice, with our protocol, we could not see any difference in LTP between CA3-CA1 synapses in the *str. radiatum* or the *str. oriens*.

Preliminary behavioral analysis of Gria1/3$^{\Delta Fb}$ mice

In Heidelberg, the behavior of the *Gria1/3*$^{\Delta Fb}$ mice was first analyzed in simple behavioral tests in male mice between 60<P<150. All experiments were performed in parallel with two age-matched control groups. One control group consisted of male littermates of *Gria3*$^{f/f}$ mice that did not contain the tTA transactivator to evaluate behavioral deficits arising from the suppression via the floxed target alleles and/or leakiness of the Cre-transgene. Another control group consisted of age-matched male C57BL/6N mice. Since both control groups exhibited similar behavior in all tests in Heidelberg, we used only the comparison to the control littermates in the detailed behavior analysis of a second cohort that was sent to Oxford (see Extended Behavioral Analysis below).

Wire-hanging (grip strength)

Mice were placed with their forepaws gripping the middle of an 18 x 21 cm^2 metallic wire mesh panel that was suspended 30 cm above the floor. The latency to fall was measured with a maximum trial time of 2 min.

Accelerating rotarod

Motor coordination and balance were tested using the accelerating rotarod apparatus (Ugo Basil). Mice had to walk on a turning rod (3 cm in diameter) that accelerated from 4 to 40 rpm within 5 min. Mice received 3 trials a day for 5 days with an inter-trial interval (ITI) of approximately 45 min. The latency to fall from the rod was measured.

Novel open field

The activity in a novel open field was monitored in a big open field box consisting of a 62 x 62 x 20 cm^3 enclosed perspex acrylic glass arena without any bedding. The total distance travelled, the pattern of movement, and the total number of rearing behaviors were video recorded (TSE-System) for 5 min.

Conditioned passive avoidance task

The passive avoidance test was performed with slight alterations to the described protocol.[98] The animal was placed in a 6 x 3 cm^2 aversive light compartment, 30 cm from the ground, facing the entrance to the 21 x 21 x 14 cm^3 dark compartment. After the animal entered the dark compartment (Timepoint: 0 hr), a mild foot shock of 0.9 mA (100V) was delivered for one second, followed 10 sec later by a second shock. 24 hr later, the animal was replaced back into the light compartment and the latency to enter the dark compartment was measured, with a maximum trial time of 2 min.

Extended behavioral analysis of Gria1/3$^{\Delta Fb}$ mice

Testing was carried out in a separate cohort of control (n = 7) and *Gria1/3*$^{\Delta Fb}$ knockout (n = 10) male mice (bred and genotyped at the Max Planck Institute for Medical Research, and imported to Oxford at 3–5 months old). All mice were single housed to prevent fighting, and a 12-h light-dark cycle was maintained (lights on at 7 a.m., lights off at 7 p.m.). Testing was conducted during the light phase. After a week of getting used to the experimenter and the experimental room, species-specific behavior was first monitored (see: Tables S1 and S2 and supplemental methods). For appetitively motivated tasks, mice were then put on a restricted feeding schedule and maintained at 90% of their free-feeding weight during testing. They were also handled and habituated to the experimenter, and to drinking the sweetened condensed milk reward (diluted 1:1 with water) in their home cages prior to testing. They were then habituated to drinking the milk from wells on a wooden feeding platform in their holding room (i.e. not the experimental testing room). An age-matched batch of C57BL/6N male mice (Harlan), which had either undergone complete bilateral cytotoxic hippocampal lesion surgery (n = 10), or were sham-operated (n = 7) were run alongside the control and *Gria1/3*$^{\Delta Fb}$ mice at the same time, and were included in some of the analyses [some of these results obtained with these hippocampal-lesioned mice were previously published in the Supplementary Information in Bannerman et al. 2012[45]].

Burrowing

This test is sensitive to both hippocampal and prefrontal cortex lesions in mice,[99,100] and as such, it forms a useful assessment for genetically-modified animals.[101] Burrowing was conducted using grey plastic cylinders, 20 cm long and 6.8 cm in diameter. These were sealed at one end and supported at the other by 2 metal legs 4.8 cm long. Each burrow was filled with 200 g of normal diet food pellets (Special Diets Services) and placed in a new cage with a thin layer of clean bedding on the cage bottom. Water was provided *ad-lib*, but no food was present in the hopper. Mice were placed individually in a cage with a burrow approximately 2 hr before the start of the dark phase of the light/dark cycle. The food remaining in the burrow after 2 hr was weighed and recorded, and the amount displaced (burrowed) was calculated. The test continued overnight without replacing the already burrowed pellets. The pellets remaining in the tube were then re-weighed the following morning (approximately 16 hr after the previous reading), and the burrowed amount was calculated. The amount of food eaten per mouse overnight (2–4 g) was a very small proportion of the 200 g in the burrow and was assumed to be similar in each group.

Nesting

Nest-building behavior is sensitive to lesions of the hippocampal, septal and medial preoptic areas.[99,102] Like burrowing, nesting is a highly sensitive test that is an important part of assessing the behavioral phenotype of genetically modified mice.[103] Mice were given clean home cages, and two squares of pressed, white cotton ('Nestlet', Datesand Ltd.), from which they could make nests, were placed in each cage. Mice were left overnight, and the nests were examined the following morning and scored as follows: 1 = no visible nest site, Nestlet untouched; 2 = sawdust in crater form, but minimal tearing of Nestlet; 3 = sawdust formed into crater and substantial tearing of Nestlet but no identifiable nest site; 4 = an identifiable, but flat nest; 5 = Nestlet completely shredded and formed into a round nest which would totally cover the mouse. This test was repeated the following night to ensure the accuracy of the score.

Hyponeophagia

This test assesses anxiety by using the mouse's natural hesitance to eating a novel foodstuff in a novel place. Animals with lesions in the hippocampus, amygdala, subiculum, or nucleus accumbens show decreased levels of hyponeophagia.[99,104,105] In test 1, the apparatus consisted of a white, 30 cm^2 Perspex base with a metal food well fixed to it at one end (1.2 cm diameter, 0.9 cm high) and a translucent plastic jug, 15 cm in diameter, with a protruding spout. The well was filled with a solution of sweetened, condensed milk (Nestle) diluted 50:50 with water. All mice were food deprived for one night before testing (16 hr in total), and had not had any contact with the milk prior to the test. The mouse was placed in a holding cage the same size and shape as its home cage but with a thin layer of clean bedding, for 5 min before testing. The animal was then placed on the Perspex base facing away from the well and the jug was upturned and placed over the animal with the spout over the well area. The latency to contact the well, and then to drink the milk were measured. The mouse was allowed 2 min to drink. If it did not drink, it was returned to its holding cage and re-tested approximately 6 min later. The mouse was re-tested a maximum of 2 times, and thus was allowed 6 min in total to drink the novel food. In test 2, mice were assessed in a different hyponeophagia test which consisted of a Perspex tube

40 cm high and 15 cm in diameter, a white plastic tray, 45 cm by 30 cm, and 45 mg Noyes pellets (Sandown. Scientific). All mice were food deprived for one night prior to testing (16 hr in total). The mouse was taken to the testing cubicle and left in its holding cage for 5 min. The Perspex tube was placed onto the white plastic tray to create an enclosed circular area and the 45 mg precision food pellets (P. J. Noyes Inc.) emptied into the tube such that they covered approximately half the floor area. After 5 min the mouse was placed into the Perspex tube by its tail and dropped the last few centimeters onto the Noyes pellets. The time taken to start eating any of the pellets was recorded. Data were combined with the previous hyponeophagia test and analyzed using a two-way repeated measures ANOVA.

Light-dark box

The Light-Dark box was developed by Crawley (1981) to assess anxiolytic drug effects.[106] Since then, it has been developed as a standard approach/avoidance conflict test of anxiety in rodents using time spent in the light section as a measure of anxiety and the number of crossings between the two compartments as a behavioral indicator of locomotor activity.[107] The apparatus comprised a wooden box with an open, white-painted section measuring 30 x 20 x 20 cm^3. This was the light compartment which had a transparent acrylic panel on one side to enable observation of the animal. It was separated by a partition (with a 10 cm x 5 cm door) from the dark compartment, painted black with a lid, measuring 15 x 20 x 20 cm^3. The aversiveness of the white compartment was increased by additional illumination from a 60W anglepoise lamp placed 45 cm from the floor of the box. The mouse was placed in the middle of the dark side, facing away from the door. The latency to cross (with all four feet) to the light portion, time spent in the dark side, and the number of transitions through the door were measured. The total time allowed was 5 min. The apparatus was cleaned between subjects with a moist, then a dry tissue. The apparatus was given a low-level mouse odour by putting some non-experimental mice in prior to commencement of testing.

Multiple static rods

This is a test of motor function and coordination as the animals not only have to travel along a static rod but they must orientate themselves through 180° and balance on the rods to do so.[108–110] The multiple static rods consisted of five 60 cm long wooden rods of decreasing diameters (rod 1, 3.3 cm; rod 2, 2.7 cm; rod 3, 2.1 cm; rod 4, 1.4 cm; rod 5, 0.8 cm). Each rod was perpendicularly screwed at one end to a supporting beam. The apparatus was elevated 60 cm above a soft surface. Previous tests with this apparatus have shown that if placed facing the exposed end of the rod, animals spontaneously orientate through 180º and run to the refuge provided by the supporting beam at the end of the rods.[111] Each animal was placed 2 cm from the exposed end of the rod, facing away from the supporting beam. Latencies to (i) orientate towards the supporting beam (a 180° turn) and (ii) travel the 60 cm to the supporting beam were recorded. A 3-minute limit was allowed and any mouse that failed to orientate or cross within this time was not tested further and allocated latencies of 180 s for the untested rods. If the mouse turned upside-down to travel or hang beneath the rod this was also noted, as was a fall from the rod. Mice were placed on the rod with the largest diameter first (rod 1), proceeding to the next, smallest rod if they completed the trial in less than 3 min.

Horizontal bar

This test assesses forelimb muscular strength and coordination.[109,112] The apparatus consisted of a 0.2 cm thick and 38 cm long metal bar, attached horizontally between two supports 49 cm above a padded bench surface. The animals were held by the tail, placed with their front paws in the middle of the bar and quickly released so that they grasped the bar. The latency to fall from the bar was recorded, with a 30 s maximum time. If the mouse traveled along the bar to either support it was allocated a time of 30 s. Latencies were then assigned a score for analysis: falls between 0 and 5s = 1, 6-10s = 2, 11-20s = 3, 21-29s = 4 and holding on for 30 s/reaching either end support bar = 5. The categorical scores from this task were analyzed with a Mann-Whitney Rank Sum test.

Spontaneous alternation

A grey wooden T-maze was used for this task, with all arms measuring 30 cm long, 29 cm high and 10 cm wide.[64] The mouse was placed in the start arm, facing the end wall, and allowed to enter the goal arm of its choice. The sliding door was then lowered and the animal was contained within the goal arm for 30 s. After this time, the animal was removed from the arm, both goal-arm doors were raised again and the central partition was removed. The animal was then placed back in the start arm, facing the end wall and allowed to choose again. This comprised one trial. The choices made by each animal on both the sample and the following choice run were recorded to establish the rate of alternation. Each animal was given 10 trials per day on 2 days, one week apart. They received 20 trials in total. The inter-trial interval on each day was approximately 15 min.

Spontaneous locomotor activity

The activity of *Gria1/3*^{4Fb} mice was recorded by the number of infrared beam breaks in a homemade photocell activity cage. Each mouse was individually placed in a 26 x 16 x 17 cm^3 transparent plastic cage with a ventilated lid that resembled a home cage in size and design. Two infrared beams crossed the cage 1.5 cm above the floor, with each beam 7 cm from the center of the cage. A thin layer of bedding (0.5 cm) was provided on the floor of each cage to reduce anxiety and encourage exploratory behavior. Mice were left undisturbed in a quiet room for 2 hr with the light on, and the number of beam breaks made by each mouse was recorded in 24-time bins of 5 min. The number of crossings, defined by the interruption of both light beams in succession, was also recorded as an indication of movement from one end of the cage to the other.

Ethological tests of anxiety

The anxiety of these animals was assessed using a battery of tests, including the Successive Alleys test, the Light/Dark Box and the Food Hyponeophagia test (see also Table S1).

Successive alleys

The successive alleys test is an approach/avoidance conflict test which is similar to the Elevated Plus maze task in how it measures anxiety but has the advantage that its linear form makes interpretation easier and also creates more of a range of anxiogenic areas. The successive alleys test was performed as described.[99,111]

Memory tests

The memory tests were performed after the basic test battery was finished. At that time, all animals were fully grown and between 4 and 8 months old.

Appetitive Y-maze task

Spatial reference memory was examined using an elevated Y-maze made of black painted wood as described previously.[27] In the elevated Y-maze, a target arm (defined according to its given spatial location relative to the room cues) was designated for each mouse to receive its 0.1 ml milk reward. Target arms were counterbalanced with respect to the group such that approximately equal numbers of knockout, control, lesion- and sham-operated animals were trained to each of the three arms. For 10 days, animals received 10 trials per day. During the eleventh session, by which point the control, *Gria1/3*$^{\Delta Fb}$ and sham-lesioned animals had acquired the task and were showing a strong preference for the baited arm, the milk reward was delivered to the food well only after the mice had made a correct choice (post-choice baiting). This was done to ensure that the mice were not simply solving the task by smelling the milk reward. Data were analyzed in blocks of 10 trials.

T-maze rewarded alternation

Spatial working memory was assessed using an elevated wooden T-maze.[27,64] Mice were run in batches of approximately 11 mice in a round-robin fashion, thus the ITI was approximately 10 minutes. Mice received a total of 10 blocks of 5 trials. For analysis, data were combined into 5 blocks of 10 trials.

Spatial reference memory in the radial maze

Spatial memory was also assessed using a six-arm radial maze that was made of grey-painted wood. Mice were trained on a radial-maze task in which the same 3 of 6 arms were always baited. The 3 baited arms were allocated such that 2 of the 3 arms were adjacent, and the third was between two non-rewarded arms (e.g. arms 1, 2, and 4). Different combinations of arms were used as much as possible, although the arm allocations were counterbalanced across groups as described.[28,45] Once an arm had been visited, this arm was blocked by Perspex doors for all subsequent choices during that particular trial.

Spatial reference and working memory in the radial maze

The hippocampal-lesion and sham-operated mice were not run on this next stage of the task as the hippocampal-lesioned mice had failed to learn the spatial reference memory component of the task. The procedure was carried out in roughly the same manner as the reference memory acquisition above, using only the *Gria1/3*$^{\Delta Fb}$ mice and their corresponding controls. Each animal had the same 3 arms baited as before. The only exception is that all the Perspex doors were raised for every choice, giving the mice a free choice between all arms. The animals were still contained in the central platform area for 10 s after visiting each arm. This procedure allowed the animals to re-enter arms that they had already visited on that trial and thus three types of error were recorded, reference memory errors –visiting arms never previously baited; working memory –correct errors – re-visiting arms that were previously baited but already visited on that trial; and working memory – incorrect errors – revisiting arms never previously baited. Animals received 4 trials per day for a further 8 days. Data were analyzed in blocks of 4 trials.

The Morris water maze (MWM)

Spatial reference memory was also assessed in an open field water maze as described in detail in several previous publications.[27,45,60] In order to escape from the water, mice had to find a fixed location, hidden platform (diameter 21 cm) submerged approximately 0.5 cm below the opaque water surface. Mice were placed into the pool facing the side wall at one of 8 start locations (nominally N, S, E, W, NE, NW, SE and SW; chosen randomly across trials), and allowed to swim until they found the platform, or for a maximum of 90 sec. Mice received 4 trials per day for 9 days, with an ITI of approximately 15 sec. On the seventh (24 hr after spatial training trial 24) and tenth days of testing (24 hr after spatial training trial 36), a probe trial was conducted to determine the extent to which the mice had learned about the spatial location of the platform. The platform was removed from the pool and the mice were allowed to swim freely for 60 sec. The percentage of time that animals spent in each quadrant of the maze was recorded. The *X* and *Y* coordinates of the animals' position during each session were sampled in real-time at 10 Hz by an Acorn computer, using specialized software that provided measures of latency, swim speed and path length during acquisition.

QUANTIFICATION AND STATISTICAL ANALYSIS

In all figures, the number of animals (n) and the number of recorded data points (n) are given as appropriate. In bar graphs, all data points used are pictured together with the standard error of the mean (SEM). In the figure legends, the tests used for statistical evaluation (ANOVA, t-test, etc.) are stated together with the P-values of the results. P-values less than 0.05 indicating a significant difference are given directly in the figures as stars. Due to space limitations in the main figure legends, detailed descriptions of the statistical analyses of the mouse behavior can be found in Tables S1 and S2. When multiple comparisons were used to control the familywise error rate, we indicate the statistical test used. When appropriate, non-parametric analyses (e.g. Mann-Whitney U-test) were conducted.